

PETROLEUM RESIDUALS IN PREBAKED CARBON ANODE BINDERS

By

M. B. Dell

Alcoa Research Laboratories
New Kensington, Pa.

INTRODUCTION

In the Hall-Heroult Process for producing aluminum, alumina dissolved in molten cryolite at 950-1000°C is electrolyzed using a carbon lined cell as cathode and baked carbon as anode. Anodes are made by mixing about 18 per cent binder with 82 per cent carefully sized calcined petroleum coke and molding a green block, which is subsequently baked at 1100° in an inert atmosphere to coke the binder.

During electrolysis the anode is slowly consumed. Carbon consumption is caused by: (1) combination of carbon with the oxygen released at the anode, (2) further combination of carbon with CO₂ initially formed, (3) air-burning of the exposed top of the anode, and (4) disintegration caused by particles of petroleum coke falling into the bath if the binder coke is more reactive than the petroleum coke. All but the first are strongly affected by the reactivity of the carbon anode, and this in turn is dependent on the quality of the coke formed by the binder.

Numerous tests have been proposed for characterizing binders. They have been reviewed comprehensively by Thomas³ and somewhat more critically by Weiler⁴. It is generally agreed that the binder should meet a softening point requirement for ease of processing, must have a low ash content to prevent contamination of the bath and also to avoid catalyzing carbon reactivity, and should be low in sulfur because of corrosion problems. In addition, high aromaticity¹ is desirable to form a less reactive anode with good electrical conductivity. Coke-oven pitch derived from coal is very aromatic and meets all these requirements. It is the binder used almost exclusively in the United States. We have now found that certain less-aromatic materials, such as those derived from petroleum, can be blended with coke-oven pitch to produce anodes equivalent in all significant properties to conventional anodes.

ANALYTICAL PROCEDURES

Softening Point

Cube-in-air method. Barrett Test No. D-7, Allied Chemical and Dye Corporation, New York, New York.

Reactivity

Sodium sulfate reactivity is the loss in weight on immersing a 1-in. cylinder of carbon 0.5-in. long for 30 minutes in sodium sulphate at 980°C. Carbon is oxidized by molten sodium sulphate². A reference carbon containing a standard binder is always run with this test for comparison. Both results are reported here since for some of the earlier tests the procedure was modified slightly.

Infrared Index of Aromaticity

This is taken as the ratio of the aliphatic transmittance at 3.4 microns

Infrared Index of Aromaticity

divided by the aromatic transmittance at 3.3 microns as previously described¹.

Discibility Test

This test measures the compatibility of a binder with coke-oven tar. A 1:1 mixture of the binder under test and coke-oven tar is heated about 30 degrees above the softening point. A small droplet is transferred to a warm glass microscope slide on a hot plate and covered with a cover glass. While still warm, slight pressure is applied to the cover glass to reduce the film thickness so that it will transmit light. When viewed under the microscope at 200X, absence of flocculation of the C-I particles normally present in coke-oven pitch indicates compatibility of the binder.

RESULTS AND DISCUSSION

A typical analysis of coke-oven pitch binder for prebaked electrodes is given in Table I. The softening point corresponds to about 215-233°F ring-and-ball.

TABLE I

TYPICAL PROPERTIES OF COKE-OVEN PITCH BINDERS FOR PREBAKED ANODES

Softening point, cube-in air	105-115
Sulfur, %	0.5
Ash, %	0.1
Infrared index	1.3

For carbon anodes made with unblended binders, the reactivity increased with decreasing aromaticity of the binder as measured by infrared index (Figure I). On the basis of infrared index binders may be divided somewhat arbitrarily into three aromaticity classes: high (>1.2), intermediate (0.6 to 1.2) and low (<0.6).

High Aromaticity Binders

Coke-oven pitch is about the only member of this class. In prebaked anodes almost any high-temperature, coke-oven pitch can produce a good anode.

Intermediate Aromaticity Binders

Pitches derived from vertical retort tars or oil-gas tar, and petroleum residuals from high temperature cracking processes fall in this class.

Low Aromaticity Binders

Among these are pitches derived from low-temperature coal tar, solvent extracts of petroleum and most petroleum residuals.

In general low and intermediate aromaticity binders do not produce good anodes and are not used alone in carbon anodes. In the United States a very minor amount of oil-gas pitch is used in 50:50 blends with coke-oven pitch.

Low Aromaticity Binders

In a search for low cost binders derived from petroleum, several residuals were found which unexpectedly produced good anodes in blends. Typical laboratory results are presented in Table II, and similar good results have been obtained in plant operation for several of these binders.

All intermediate aromaticity binders tested produced good anodes when blended with coke-oven pitch. These results were not unexpected since blends of oil-gas pitch have been used for some time in anodes. Recently residuals produced in petroleum processing by high-temperature cracking have become available. Those having intermediate aromaticity (A and B in Table II) should find application blended in anode binders. None of the petroleum residuals tested had aromaticities as high as coke-oven pitches.

Certain low aromaticity binders when blended with coke-oven pitch produced good binders. These included a petroleum residual (C - Table II) produced by propane deasphalting of an Ordovician crude and a pitch (D) derived from low-temperature lignite tar. Other low aromaticity binders, such as air-blown asphalt (E in Table II), produced poor binders. The only laboratory test which differentiated among these binders was the miscibility test. Those blends in which the C-I particles were flocculated produced poor binders (E and F in Figure 2). If the C-I particles remained uniformly dispersed (A and C in Figure 2) the blend produced good anodes.

While some of these binders did produce good anodes, their true coking values were lower than that of coke-oven pitch (Table II). This did not seem to affect their utility, but their economic value was lowered since less carbon would be available for reaction with oxygen produced at the anode in smelting cells.

CONCLUSION

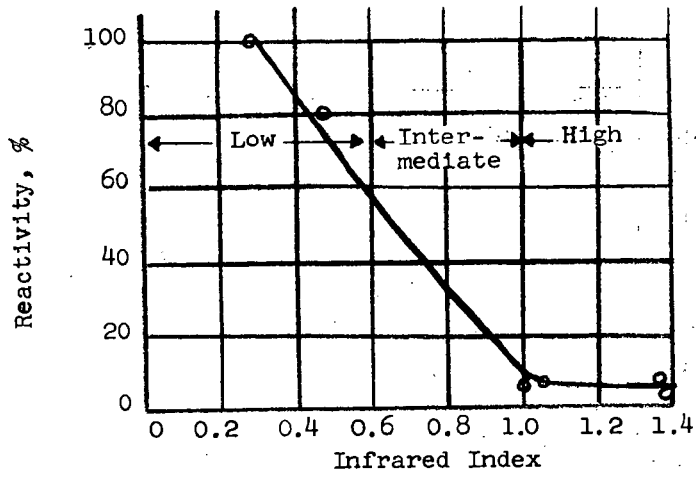
High aromaticity binders can be used alone to produce good anodes. Intermediate aromaticity binders blended with coke-oven pitch produced good anodes. In blends low aromaticity binders which were miscible with coke-oven pitch produced good anodes.

REFERENCES

1. Dell, M.B., FUEL 38, 183 (1959)
2. Fotiev, A.A., Zh. Prikl. Khim. 35, 2402-9 (1962)
3. Thomas, B.E.A., Gas World, Coking Supplement 51-66 (April 2, 1960)
4. Weiler, J.F., "Chemistry of Coal Utilization", Lowry, H.H. - ed. Supplementary volume, John Wiley & Sons, Inc., New York, 1963 P. 627

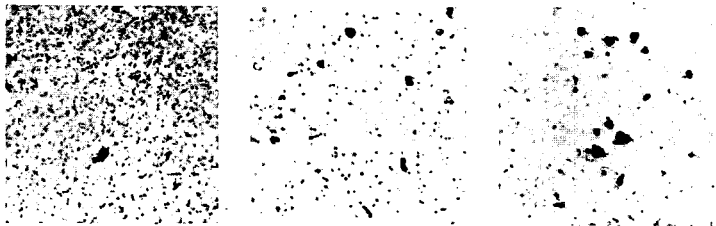
TABLE II
BINDER BLENDS IN LABORATORY PREBAKED ANODES

Binder	Source	IR Index	Coke-Oven Pitch in Blend, %	Binder %	Actual Coking Value, %	Anode Properties Resistivity ohm-in.	Anode Properties Reactivity %
A Reference	Pet. therm. Process Coke-oven pitch	1.07	50 100	18.5 17.5	52.7 64.2	0.0024 0.0023	11.9 22.6
B Reference	Pet. therm. Process Coke-oven pitch	0.78	60 100	17.5 17.5	55.9 68.8	0.0021 0.0022	33.6 57.0
C Reference	Pet. propane deasphalt. Coke-oven pitch	0.3	50 100	17.5 17.5	49.7 63.4	0.0023 0.0026	30.1 46.8
D Reference	Lig., low-temp. carb. Coke-oven pitch	0.14 1.36	60 100	18.5 18.5	- -	0.0026 0.0025	6.7 5.6
E Reference	Pet. air-blown Coke-oven pitch	0.11 1.32	50 100	18.5 18.5	- -	0.0035 0.0022	9.3 4.5



Reactivity of Laboratory Prebaked Anodes

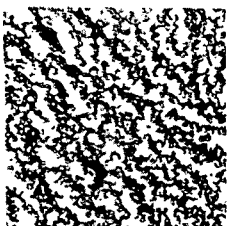
Figure 1



100% Coke

50% - C

50% - A



50% - F

50% - E

Miscibility Test Micrographs of Coke Oven Pitch Blends (Transmitted Light, 200X)

Figure 2

Aspects of the Reactivity of Porous Carbons with Carbon Dioxide

J. H. Blake (a), G. R. Bopp (b), J. F. Jones (c), M. G. Miller (c), W. Tambo (d)

(a) Chemical Engineering Department, University of Colorado

(b) Present address, Chemical Engineering Department, Stanford University

(c) FMC Corp., Chemical Research and Development Center

(d) Present address, Cabot Corp., Boston, Massachusetts

I. Introduction

This work was undertaken in order to develop a simple and effective test that would compare the reactivities of granular carbons. The carbons studied were samples of formed metallurgical coke and of calcined coal char made from subbituminous coal in the process developed by FMC Corp., and demonstrated in a semi works plant at Kemmerer, Wyoming (1). This coke is permeated by a system of very fine pores, it has a highly amorphous solid structure, and it is very reactive compared to byproduct or beehive cokes. The reactivity is believed to be an important property of cokes used as reducing agents.

As a second objective, some knowledge of the influence of rather mild thermal treatment on the reactivity of these cokes was sought.

Carbon dioxide was selected as the oxidizing agent for the reactivity tests, since its reaction with carbon is not complicated by secondary effects such as the water gas shift. The reaction was followed by measuring the weight of carbon as a function of time, and this procedure proved to be both simple and precise.

While the variables affecting the results of the test were studied in a semi-empirical manner, certain interesting information regarding the kinetic behavior of these carbons as they underwent reaction did result, and this work is presented with the hope of providing a lead toward a better picture of what happens on the surface of carbon during reaction.

II. Experimental Details

A. Reactivity Measurements

The apparatus shown in Figure 1 consisted of an impervious silica tube 2.54 cm. I D mounted vertically in a tube furnace. Carbon dioxide flowed upward through the tube at controlled rates which ranged from 2870 cc per minute (STP) to 4730 cc per minute. The samples of granular carbon to be evaluated were suspended in a sample holder from an analytical balance mounted above the reaction tube. The sample holder was a No. 2 Gooch crucible cut off where the outside diameter was 23 millimeters so that clearance between the crucible and the reaction tube averaged 1.2 mm. The perforations in the bottom of the crucible were each .7 mm Diam. Holes were cut in the sides of the crucible with a diamond saw so that a bale of quartz fiber which hooked on to another long quartz fiber attached the sample holder to the balance.

Nearly all of the reactivity measurements were made at 900°C and the temperature was controlled automatically by the thermocouple mounted about 1 cm below the sample. At 900°C, the rates of reaction of most of these samples were in a range that was convenient to follow.

A loose fitting cover on top of the reaction tube with a small hole for the quartz fiber prevented air from diffusing down to the sample yet permitted the CO₂ to escape.

The dynamic force or upward drag on the sample basket was about 50 milligrams at the highest gas velocity used, and it was steady as long as gas velocity and temperature were kept constant.

To make a reactivity measurement the carbon particles were screened, usually to -16 +20 USS mesh, dried overnight in a desiccator and a sample of either 200 or 500 milligrams was weighed into the sample holder. With the apparatus at reaction temperature and thoroughly purged with nitrogen, the sample holder was quickly lowered into place, hung from the balance, and the cover placed on top of the reaction tube.

The sample was then allowed to heat in a stream of nitrogen until it came to a constant weight, which usually happened within ten minutes, but for most runs a 20 minute devolatilization period was used. At the end of this time the weight was observed, the carbon dioxide was turned on and its flow adjusted to give a superficial velocity of either 15.6 or 9.45 centimeters per second (STP) in the reaction tube. The weight was again measured as soon as possible after turning on the CO₂ and thereafter at frequent intervals during the course of the reaction. At the end of the run the system was purged with nitrogen, and the sample was removed and allowed to cool to room temperature. The empty sample holder was then placed back in the furnace and weighed in a stream of nitrogen at reaction temperature. Reactivities are reported as percent of the sample reacting per hour, based on the total weight (including ash) of carbon at the end of the devolatilization period.

For most of the work the lower gas velocity, 9.45 cm/sec, was used because it gave somewhat more reproducible results. At this velocity, the Reynolds Number in the annular space past the sample is 900, so that flow is laminar.

B. Fluidized Reactor

The apparatus to react carbon with steam in a fluidized bed consisted of an impervious silica tube 2.54 cm I D mounted vertically in a furnace. The heated section of the tube was 45 cm long, and it contained refractory packing to a depth of 25 cm to preheat the steam. A perforated porcelain plate pinched into a constricted section of the tube lay on top of the packing and served as a grid. A thermocouple in a fine quartz well was immersed in the bed from the top, and it operated a controller which acted to maintain a constant temperature in the bed.

The rate of steam flow was controlled by manual adjustment of the current to a heating mantle enclosing a two liter flask. The flask was filled to a level well above the windings in the mantle.

To begin a run, the empty reaction tube was weighed, then mounted in the furnace, brought up to temperature, and the steam flow was adjusted to the proper rate. The weighed carbon sample (20 grams) was then poured into the tube, and a plug of glass wool was inserted into the top. By proper manipulation of the heater, the bed temperature reached the desired value (usually 750°C) within 5 minutes.

Coarse carbons, -6 +10 USS mesh, were used for this work. At a superficial steam velocity of 25 cm/sec under reaction conditions, particles in the bed moved

about continuously. Thus each particle should have been exposed to the same conditions. The beds were about 5 cm deep.

C. Surface Area Measurements

A Perkin-Elmer-Shell Sorptometer (Model 212) was used to measure pore surfaces. Samples were degassed in the apparatus at 600°C under .1 mm Hg for 30 minutes.

Isotherms for adsorption of nitrogen at 78°K were obtained by a flow technique which is rapid, but which may not allow sufficient time for equilibrium to be attained in very fine pores. Thus the surface areas reported here may be somewhat low.

D. Particle Density and Pore Volumes

Particle densities or volumes were measured by displacement of Hg at 10 psig in an American Instrument Co. Porosimeter. Pressures to 5000 psi enabled pore volume distributions to be determined down to pore diameters of 350A.

E. Helium Densities

Helium density was measured in a Beckman purgeable gas pycnometer, after degassing in the apparatus at room temperature and .1 mm Hg twice for about 10 minutes each time, and breaking the vacuum with He in each case.

F. Heat Treatment of the Samples

To study the effect of heat treatment on reactivity the carbons were soaked for various periods of time in a muffle furnace kept at either 1000°C or 1100°C. During this soaking, whole briquets were contained in glazed porcelain crucibles with calcined coal packed around them and with covers on the crucibles.

III. Samples

Two samples of FMC Coke briquets and one sample of calcined coal char were studied in this work.

The coke briquets were made in pilot scale equipment by first calcining the ground coal in a series of fluidized retorts, then briquetting the devolatilized coal or calcinate with a binder made by air blowing the tar distilled from the coal. The green briquets were then cured in the presence of air to polymerize the binder, and were finally coked or baked at about 900°C.

One sample of coke was made from Elkol Coal, a sub-bituminous coal mined near Kemmerer, Wyoming. The other coke was from another sub-bituminous coal mined near Helper, Utah.

For the samples used here, coke briquets were crushed and screened to the desired size.

The sample of calcinate was made from Elkol Coal and was produced by FMC Corp's demonstration plant at Kemmerer, Wyoming. The pulverized coal was first dried at 150°C, then carbonized at 450°C, and finally calcined at 800°C in a series of fluidized retorts.

Properties of these carbons are given in Table I.

TABLE I
Properties of Samples

	<u>Elkol Coke</u>	<u>Helper Coke</u>	<u>Elkol Calcinate**</u>
Ultimate Analysis			
Wt. % C	89.8	86.6	89.6
H	1.0	1.0	1.3
N	1.0	1.2	1.2
S	.6	.3	.4
O (by diff.)	1.7	2.6	1.7
Ash	5.9	8.3	5.8
Volatile matter %	2.0%	2.0%	4.5%
Surface area (m ² /gm) BET-Nitrogen	240*	170	190
Apparent density by Hg displacement (gm/cc)	.94	.96	.94
Helium density (gm/cc)			1.98
Crushing strength of cylinders 1-1/4" x 3/4"	3400#	3400#	

*190 m²/gm is a typical surface area for the coke produced by the large-scale plant at Kemmerer.

**The Elkol Coke used here was not made from this sample of calcinate.

IV. Results

A. Effects of Procedure

Several of the possible variables of this apparatus were studied to determine their effects on the reactivity measurements and to establish a standard procedure. The Elkol coke was used for this aspect of the work.

The numerical rates or reactivities reported in this section are based on the overall slope of the weight versus time curve between the times of 30 and 160 minutes where the slope was fairly constant. In the first few minutes of reaction, rates were somewhat higher than the slope in this interval, and the possible significance of this higher initial rate is discussed in a later section.

Table II shows the effects of sample size, devolatilization time, gas velocity, and particle size on the measured values of reactivity. In brief, increasing the sample size from 200 to 500 milligrams decreased the reactivity about 20%; longer devolatilization times (40 compared to 20 minutes) decreased the reactivity roughly 10%; and decreasing the gas velocity from 15.6 to 9.45 centimeters per second lowered the reactivity about 20%. Particle size between -6+10 and -28+32 mesh had no appreciable effect. (These screen sizes cover a five fold range of average particle size, from 2.5 down to .5 millimeters.)

TABLE II
Variables Affecting Reaction Rate*

Particle Size	Heating time min.	Sample Wt. mg.	Gas Velocity cm/sec	Reaction Rate %/hr	Comparison of Variables
-16+20	20	200	15.6	25.6	Sample Weight Heating Time Gas Velocity
		500		25.1	
		500		26.4	
	40	200		20.1	
		200		21.4	
		500		20.2	
- 6+10	20	500	9.45	24.1	Particle Size
				24.1	
				18.3	
	40			18.4	
				17.6	
				17.2	
-16+20	20	500	9.45	17.8	
				17.7	
				18.2	
-28+32	20	500	9.45	17.6	
				17.8	
				17.9	

*(Elkol Coke)

The procedure adopted as standard used the -16+20 mesh size range, a heating time of 20 minutes, 500 mg. of sample and a gas velocity of 9.45 cm/sec. Reproducibility under these conditions was good, as can be seen from Table II.

The reactivity was reproduced with several different sample baskets made as described above, but having slightly different wall clearances. Thus the dimensions of the sample holder are not critical.

B. Effects of Carbon Monoxide

It is well known that CO and H₂ retard the reaction between CO₂ and carbon (2,3). With the sample sizes and flows of CO₂ that were used here, the average concentration of CO generated in the reactivity apparatus was usually between .1 and .2% (i.e. moles CO produced/unit time divided by moles of CO₂ fed/unit time). For the most reactive sample, the composition of CO in the effluent gas was about .45%.

Several runs with CO added to the CO₂ fed to the reactor (total flow kept constant) showed the rate to be lowered about 20% with 3.7% CO in the gas. This is about what Ergun's data (4) would predict and it shows that the CO generated by reaction should have a very minor influence on the measured values of reactivity.

C. Heat Treatment

Figures 2, 3, 4, and 5 show how the weights of carbon samples changed with time during reactivity determinations. Note that zero time has been shifted for most of the data on Figures 3, 4, and 5 so that several runs can conveniently be compared on a single plot.

From these plots, two results are apparent. First, as would be expected, a more severe heat treatment causes a given carbon to react more slowly.

Secondly, the heat treatment causes the rate of reaction to become more nearly constant, during a particular run. In Figure 2, for example, a sample of Helper coke which had been soaked at 1000°C for 16 hours reacted at very nearly a constant rate until more than 56% of the carbon had been consumed. The least-squares slope of this line to 56% burn off gives a reactivity of 38.1%/hr with 95% confidence limits of $\pm 5.1\%$ /hr. The other sample in Figure 2 was soaked for 27 hours at 1000°C and it reacted to 57% burnoff at a constant rate of $24.7 \pm 2.28\%$ /hr. The 95% confidence limits give a quantitative idea of how nearly constant these reaction rates were.

D. Effect of Temperature

Except for two runs at 850°C all of the reactivities reported here were measured at 900°C. The two runs at 850° with Elkol coke gave reactivities of 6.5 and 7.1% per hour and when compared with 17.8% per hour at 900°C the apparent overall activation energies were 58.3 and 56.0 K cal per mole, respectively.

E. Variation of Pore Surface with Burnoff

Pore surface areas and particle densities were determined for 500 mg samples of Elkol calcinate which had reacted with CO₂ for various lengths of time in the reactivity apparatus. The first part of Table III shows these data. This carbon had been heated only to 800°C before undergoing reaction, so that the rate of reaction decreased continuously with burnoff, as was the case for the "un-heat-treated" carbon in Figure 5.

The specific surface of the carbon increased more or less continuously with burnoff, but when the surface area was based on 1 gram of original sample, before reaction (Column 6), it went through a maximum at about 35% burnoff. The data, plotted in Figure 6, show that the surface of a sample rises rapidly to a maximum and then falls off as carbon is consumed. Probably, during the initial stages of reaction, additional pore surface is very quickly made available by erosion of constrictions, and perhaps by enlargement of very fine pores. However, during the later part of the reaction, beyond 35 to 40% burnoff, pore surface is destroyed more rapidly than it is created, most likely by consumption of walls separating fine pores.

It is conceivable that the actual surface accessible to the carbon dioxide or steam at reaction conditions differs greatly from that measured by adsorption of nitrogen at 78°K. However, it is hard to imagine that the pore surface available to the reactant gas can do anything but increase during the first 10 to 20% of burnoff. During this part of the reaction, the rate either remains essentially constant, or decreases gradually.

Thus during the course of reaction of a particular sample of carbon there seems to be no correlation between reaction rate and pore surface area.

The percent internal reaction from the last column in Table III gives the weight loss calculated from the particle densities, which assumes that all reaction takes place on the internal pore surface. The difference between this figure and the actual weight

TABLE III
Variation of Pore Surface with Burnoff

Time Reacted Min.	Overall Wt. Loss %	Particle Density gm/cc	Overall Rate %/hr	Specific Surface m ² /gm	Surface* Per Gm. Starting Material m ² /gm	Internal Reaction** %
Calcined Elkol Coal -20+30 Mesh Reacted with CO ₂ in Reactivity Apparatus at 900°C						
0	0	.935		190	190	
15	5.7	.934	20.7	453	430	
30	10.0	-	20.0	592	534	
45	13.9	.815	18.5	642	552	12.8
60	18.2	.765	18.2	760	622	18.2
75	21.8	.721	17.4	790	616	22.9
90	25.9	.737	17.3	930	689	21.2
105	27.4	.681	15.7	975	707	27.1
120	32.0	.686	16.0	982	668	26.6
135	34.8	.655	13.9	1165	770	30.0
150	40.7	.639	16.2	1180	700	31.7
165	41.2	.605	15.0	1229	721	35.3
180	44.1	.625	14.7	1158	646	33.1
210	44.5	.618	12.7	1108	615	33.8
240	58.9	.530	14.7	1501	616	43.3
270	60.2	.510	13.4	1581	625	45.5
300	63.1	.549	12.6	1426	526	41.3

Calcined Elkol Coal -6+10 Mesh Reacted with Steam in Fluid Bed at 750°C

0	0	.965		139	139	
30	8.0	.908	16.0	560	515	5.9
45	13.0	.873	17.4	559	485	9.5
60	20.0	.817	20.0	743	596	15.2
75	23.5	.835	18.8	801	612	13.5
75	21.5	.767	17.2	798	628	20.5
90	26.5	.702	17.7	792	583	27.1
90	28.5	.760	19.0	784	561	21.1
105	34.5	.649	19.7	942	619	32.7
105	32.5	.711	18.6	899	608	26.1
105	33.5	.731	19.2	830	552	24.1
120	35.0	.693	17.5	911	592	28.1
120	37.5	.678	18.8	712	445	29.7
135	43.5	.579	19.3	893	504	40.0
135	43.0	.645	19.1	933	532	33.1
150	48.0	.586	19.2	911	475	39.2
150	45.0	.588	18.0	968	532	39.0
165	51.2	.615	18.6	907	442	36.2
165	49.9	.494	18.1	1100	551	38.8
180	55.5	.527	18.5	964	429	35.4
180	52.0	.567	17.3	1064	511	41.3
180	56.6	.589	18.9	945	409	39.0
180	51.5	.552	17.2	942	457	42.8

* (Specific Surface) (100 - % wt. loss)/100

** 1 - (part. density)/(initial part. density)

loss represents carbon consumed on the outsides of the particles. Although the data are somewhat erratic, roughly 85% of the reaction took place on the internal surface up to 40% burnoff.

The second set of data in Table III refers to -6+10 mesh Elkol calcinate reacted with steam at 750°C in the fluidized bed. Here, at a lower temperature, the rate of reaction of "un-heat-treated carbon" is very nearly constant at 18.2%/hr with 95% confidence limits of $\pm 1.0\%$ /hr. (These measurements are less precise.) In this case also, the pore surface increases to a maximum at about 30% weight loss, and then decreases. Since there is some attrition in the fluid bed, particularly at high burnoff, the amount of internal reaction is quite a bit less than that indicated by the actual weight loss.

V. Discussion

A. Variables affecting reactivity

Several observations indicate that mass transfer is not a major factor limiting the rate of reaction in this work. First, the fact that a five fold range of particle sizes had no apparent influence argues that diffusion within the pores of the particles and diffusion from the voids in the sample bed to the surface of the particles did not cause a significant concentration gradient, and that therefore, the concentrations of carbon dioxide and carbon monoxide in the voids between particles must be essentially the same as at the pore surfaces where reaction takes place.

Second, the overall activation energy of 56 to 58 K cal is too large for diffusion to the particles to control the rate, even though this activation energy was determined between only two temperatures, and most of the data pertain to the higher temperature.

Another factor which suggests that external or film diffusion does not govern the rate is that the observed rates of reaction varied from 70% per hour to 4% per hour depending only upon the characteristics of the carbon. Thus, over this range of reactivities any effects on the diffusion rate to and from the particles by the geometry of the apparatus or the pattern of gas flow should have been unchanged.

Although diffusion of gas either to the particles or within their pores does not appear to strongly affect the rate of reaction here, its effect may not be negligible, particularly at the higher rates. If film diffusion, pore diffusion, and chemical reaction at the pore surface are regarded as three resistances to reaction arranged in series, lowering one resistance, as when the pore surface becomes more reactive, increases the relative significance of the others.

The importance of pore diffusion is undoubtedly affected by the pore structure. If a carbon is very dense, and has only very fine pores, its permeability to the reactant gas may very well be so low that reaction only takes place near the external surface of the particles. Thus the pore structure (permeability as well as pore surface area) might very well influence measured values of reactivity in this apparatus.

A further, and most likely the predominant, physical factor influencing the values of these reaction rates is that the samples were probably not isothermal. At a rate of 20% per hour, the endothermic reaction of carbon dioxide requires about 360 calories per hour for a 1/2 gram of carbon. Assuming that this heat is transferred principally by radiation, the surface of the sample was probably 2° to 4°C less than the measured temperature inside the reaction tube. With an activation energy of 58 K cal such a difference in temperature would lower the rate by a factor of 4 to 8%. This cooling effect would be more pronounced with the larger samples and at the lower gas

velocities. Therefore, the actual sample temperature and thus the measured reaction rate would be somewhat lower for larger samples and lower gas flows, as was observed.

The net result of all of these factors is that while this procedure does indicate significant differences in reactivity among various samples of carbon, the measured values are somewhat compressed. At the higher rates of reaction the combined retarding effects of diffusion, carbon monoxide, and a somewhat lowered sample temperature give a measured value of the reactivity which is less than would be the case if the sample were reacting under the same actual conditions as one with a lower reactivity. At the lower rates of reaction these inhibiting influences are not so large since concentration differences between the sample and the main stream of the gas are less, as are temperature differences. Thus these differing values of reactivity must be interpreted as occurring under conditions of reaction which are not exactly similar and where the higher rates have taken place under "slower" conditions so that the true differences in reactivity are actually somewhat greater than those reported here.

B. Concentration Gradient Inside Particles

Since, with the Elkol Coke, variation of particle size from about 2.5 to .5 mm did not influence the measured reactivity, one might conclude that reaction occurred entirely within Zone I (5) - that is uniformly throughout the particles, with a negligible radial gradient in the concentration of CO_2 .

However, the particle densities reported in Table III for Elkol calcinate show the percent of internal reaction to be consistently less than the overall weight loss, which suggests that reaction is not uniform throughout the particle.

In the case of Elkol calcinate, macro-pore volume measurements by displacement of Hg up to 5000 psi show a porosity of 28% in pores larger than 350A in diam. About two-thirds of this porosity is in pore sizes between 3000 and 30,000A. If these large pores are regarded as arteries which conduct gas to cells where the pores are much finer (the mean diameter of the pores less than 350A diam. is 25 to 30A), it should be possible to estimate whether a significant radial concentration gradient occurs in these pores.

From density profiles of carbon rods exposed to CO_2 for various times at several temperatures, Walker and co-workers (6,7) concluded that the dimensionless group $\left(\frac{R}{C_R \text{ Deff}}\right) \left(\frac{dn}{dt}\right)$ is a measure of whether reaction occurs uniformly throughout the particle in Zone I, or Zone II where the CO_2 is all consumed before it can diffuse to the center of a particle. Here R is the particle radius; C_R the reactant concentration in the main stream; dn/dt the overall reaction rate per unit particle external surface; and Deff the effective diffusion coefficient of CO_2 within the particle, all these terms being in consistent units. Deff equals $D \epsilon / \tau$, where D is the diffusion coefficient in a single cylindrical pore; τ , the tortuosity factor (estimated at 20); and ϵ the fraction of the external particle surface covered with pore openings - estimated to be 1/3 the volume porosity for pores 3000 to 30,000 A in diam.

Assuming spherical particles, a first order reaction, and no inhibition by products, if $(R/C_R \text{ Deff}) (dn/dt)$ is less than .03, reaction should be in Zone I; if greater than 6.0, the conditions of Zone II apply.

Using data from Table III and 3000 A for "large" pore diameters, estimates of this dimensionless group vary from .8 to 2.4, which indicates that while reaction occurs throughout a particle, it does so to a greater extent close to the external surface -- that is, the condition is between Zones I and II.

A question remains concerning the "cells" of fine pores surrounded by the network of large arterial channels. If the dimensionless group $\left(\frac{R}{C_R \text{ Deff}}\right) \left(\frac{dn}{dt}\right)$ is set equal

to .03, which is its maximum value if the conditions of Zone I (uniform reaction) apply, the equality can be solved for R, the maximum particle or "cell" radius for uniform reaction. Estimating values for C_R , $Deff$ (Knudsen diffusion occurs in pores 25A diameter) and dn/dt (a function of R), and solving for R gives a value of .014 cm for the calcinate used in the first part of Table III. This gives a "cell" diameter which is about half a particle diameter. Since a "cell" of this size must surely be permeated by the large pores, it is the concentration gradients in the large arterial pores which must be responsible for non-uniform reaction.

C. The Constant Rate of Reaction

Figures 2, 3, 4, and 5 show that for heat treated carbons, the weight-time plot during a considerable portion of reaction is very close to a straight line.

The fact that the kinetic order of carbon can be zero after 1 or 2% burnoff has often been observed before (8,9). The carbons discussed here were all exposed to some CO_2 or steam at 800° - $900^\circ C$ in their preparation, so this initial burnoff undoubtedly occurred prior to these reactivity measurements.

It is of particular interest to note that while the reaction rate is either constant or slowly decreasing, the pore surface first rises rapidly, and then decreases. The data for Ekol Calcinate of Table III are plotted in Figure 6.

Forty years ago, Chaney and co-workers established that the pore surface as manifested by adsorptive capacity for vapors first rises to a maximum and then falls off as a given sample of carbon undergoes activation (10).

Thus there is apparently no relation between a carbon's pore surface area and its rate of reaction with CO_2 or steam as a particular sample undergoes reaction. Even though pores may be available to the reacting gas at 750° - $900^\circ C$ which are not coated by nitrogen at low temperature in the surface area determinations, the extent of pore surface and its accessibility must certainly increase during the first 10 to 20% of reaction.

With the available surface changing as it does, the constancy of the reaction rate of these stabilized carbons is particularly striking. The explanation of a constant "porosity profile", which might well apply under conditions of Zone II (6) does not seem to apply here, where reaction is occurring throughout the particles.

In the reaction mechanism set forth by Ergun (11) an oxygen atom adsorbed on the carbon surface goes off as carbon monoxide and leaves behind either one, two or no active sites on the carbon. In the present case a single active site must be left behind on the stabilized carbon to give a rate of reaction so nearly constant. This constant rate is strong evidence that for a carbon stabilized by heat treatment, reaction of a molecule of CO_2 or H_2O with an active site on the solid to give an adsorbed atom of oxygen, and the subsequent evaporation of CO from this site must preserve or replace the active site somehow. Thus when one active site reacts, another is regenerated in its place, so that the number of active sites remains virtually the same as reaction proceeds.

This picture is a reasonable one. A reactive site probably involves an atom on an edge or a corner having one or more high energy bonds (12); when this atom is removed one of its neighbors would very likely be left similarly situated.

Studies of electron spin resonance have shown that carbons which have been heated to over $800^\circ C$ have very few unpaired electrons (at room temperature) so that the active site is probably not a surface free radical. Harker and co-workers (13) believe that in impure carbons, surface sites involving hydrogen or metallic impurities contribute more to the reactivity than do unpaired electrons. Perhaps the hydrogen and metal contents are sufficiently stable in carbon at $900^\circ C$ after treatment at 1000° or 1100° so

that the number of atoms of each remains constant during a large part of the reaction. It seems unlikely, however, that the hydrogen content would remain so precisely constant during oxidation by CO_2 , so a constant level of catalytic metallic impurities during the reaction appears to be a possibility for explaining the constant rates. This explanation would demand that a "stable" active site be associated or coupled with such an impurity, and it is certainly reasonable that a carbon atom on the edge of a graphitic crystallite might exchange electrons with a metallic atom contacting the same crystallite.

D. Effect of Thermal Treatment

Amorphous carbons usually (but not always) become less reactive upon heat treatment. The loss in reactivity with heat treatment shown in Figure 7 is therefore to be expected. The fact that reactivity plotted vs. time of heat treatment gives very roughly a straight line on log log coordinates as in Figure 7, shows that heat treatment decreases the reactivity quite rapidly at first and very much more slowly as the time of treatment is extended. The thermal soaking would be expected to permit local rearrangements or recrystallization of the carbon to anneal points of strain or perhaps to allow edge carbon atoms to orient themselves into a graphitic structure. Less reactive sites or perhaps isolated dislocations could be expected to stabilize themselves more slowly. At 1000° or 1100°C graphitization of an amorphous carbon hardly proceeds at all, and x-ray diffraction patterns of some of these heat treated carbons did not differ significantly from those of the "unsoaked" coke. Thus, while no gross recrystallization occurred in these heat treatments, it is logical to expect that very local rearrangements may have stabilized the carbon.

Figure 5 shows that the rate of reaction of the untreated or unheated Elkol coke falls off within $2\frac{1}{2}$ hours to about the same rate as coke which had been heat treated at 1000° for seven hours. This decrease in rate of the untreated sample is too much to explain by the effect of the thermal treatment alone. Neither will reaction of binder carbon in the briquetted coke at a faster rate than carbon from the particles explain this decrease, since the calcined coal particles follow practically the same reaction paths as the coke. (See Table III.)

If active sites are regenerated during reaction they must migrate around the surface of the carbon so that occasionally an adjacent carbon atom might already be active and therefore both active sites might not be regenerated on reaction. However, while this factor could very well be appreciable in the later stages of reaction it apparently is not of importance in the heat treated samples and therefore it is hard to see why it might be significant in the untreated cases.

One possible explanation for the decrease in rate with unstabilized carbon could be that there are several types of reactive sites, some of which are much less stable and more reactive than others. This concept actually is highly likely and has often been cited. These more reactive sites would be those more readily annealed by the heat treating process and if they are not always regenerated on reaction but instead are replaced by less active sites, the rapid loss in reactivity of the untreated sample could be explained. Thus the heat treated samples would probably contain not only fewer reactive sites but also sites which are of a lower and more uniform order of reactivity and which are apparently regenerated in kind by gasification.

As another possibility, stable sites might be those associated with metallic impurities, while less stable, non-regenerated sites might be those solid defects that are readily healed by annealing.

VI. Summary

The principal finding of this work is that a carbon stabilized by suitable thermal treatment reacts with carbon dioxide at very nearly a constant rate during the consump-

tion of a major portion of the sample. This occurs under conditions where the overall rate of reaction is largely governed by the chemical step.

This constant reaction rate strongly suggests that every time a reactive atom of carbon leaves the solid state as carbon monoxide, another carbon atom is made reactive. Thus, during the course of oxidation the chemical state of the carbon surface remains constant even though the physical state (shape and surface area) changes.

With the unstable carbons the reaction rate falls off faster during reaction than during heat treatment alone. Therefore the chemical state of these carbons must change during the course of reaction. A possible hypothesis suggests that when a highly reactive site is removed from the solid matrix, it leaves behind a less reactive site so that the carbon stabilizes as reaction proceeds.

It is a pleasure to acknowledge that this work was supported by FMC Corporation, and to thank J. Work, R. T. Joseph, J. A. Robertson, and C. H. Hopkins of FMC for many helpful suggestions.

BIBLIOGRAPHY

- (1) Coking Western Coals, Coal Age, pg. 90, (December 1963); Chemical Wk (17 Jan 1960).
- (2) Ergun, S., Kinetics of reactions of CO₂ and steam with Coke, USBM Bull. 598, (1962).
- (3) Walker, P. L., Rusinko, F., Austin, L. G., Gas reactions of carbon. Adv. in Catalysis XI, pg. 143, (1959).
- (4) Ref. (2) pg. 9.
- (5) Ref. (3) pg. 165.
- (6) Ref. (3) pg. 178.
- (7) Kawahata, M., Walker, P. L., Mode of Porosity Development in Activated Anthracite. Proc. 5th Carbon Conf., Vol. 2, pg. 261, (1962).
- (8) Ref. (3) pg. 161.
- (9) Walker, P. L., Foresti, R. J., Wright, C. D., Surface area studies of carbon, Ind. Eng. Chem. 45, 1703, (1953).
- (10) Chaney, N. K., Ray, A. B., St. John, A., Properties of Active Carbon, Ind. Eng. Chem. 15, 1244, (1923).
- (11) Ref. (2) pg. 13.
- (12) Bradshaw, W., Oxidation of Graphite and Various types of carbon. 6th Biennial Conf. on Carbon.
- (13) Harker, H., Jackson, C., Gallagher, J. T., Horsely, J. T., Reactivity of Carbon and Graphite: Role of unpaired electrons. 6th Biennial Conf. on Carbon.

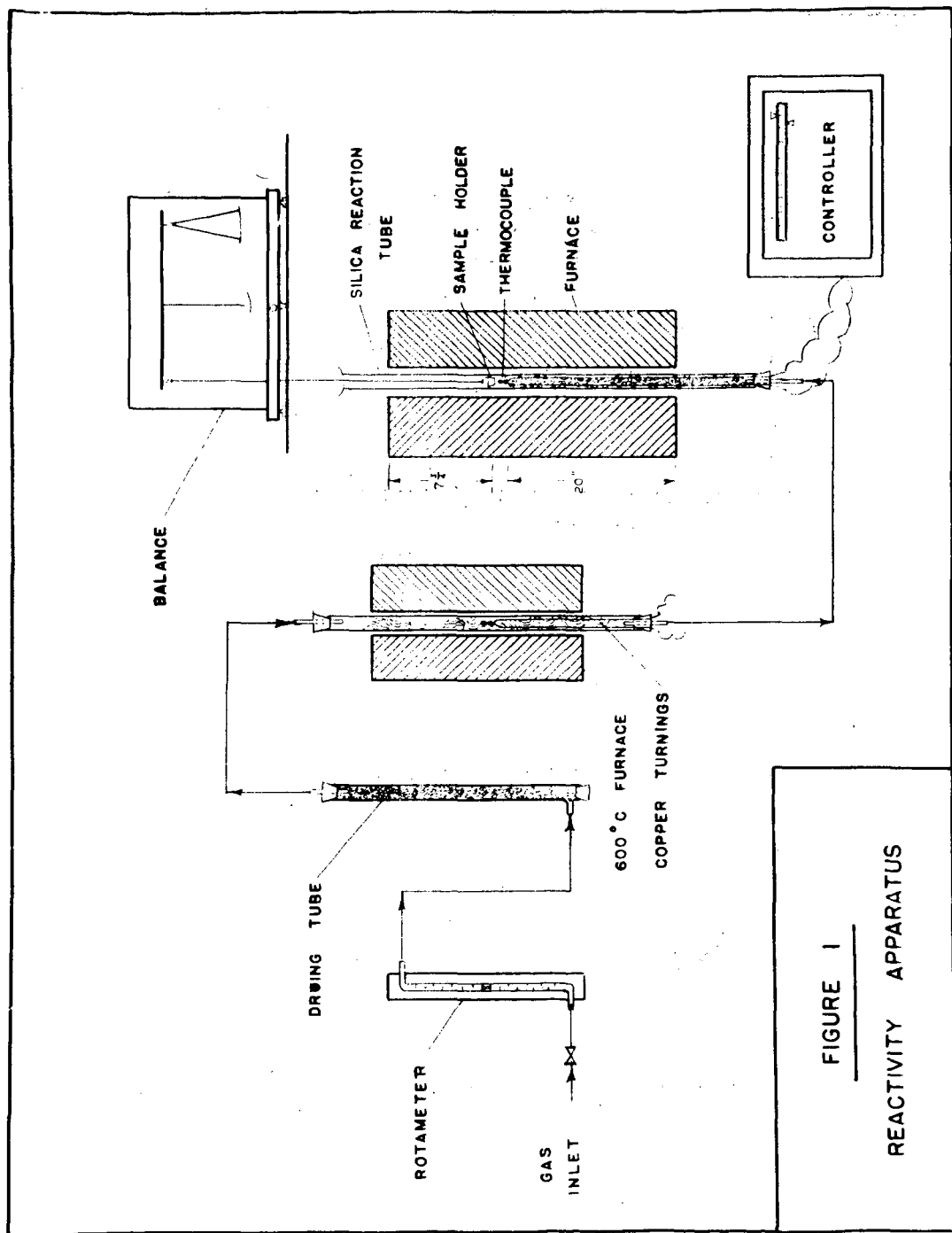


FIGURE 1
REACTIVITY APPARATUS

REACTION OF HEAT-TREATED HELPER COKE

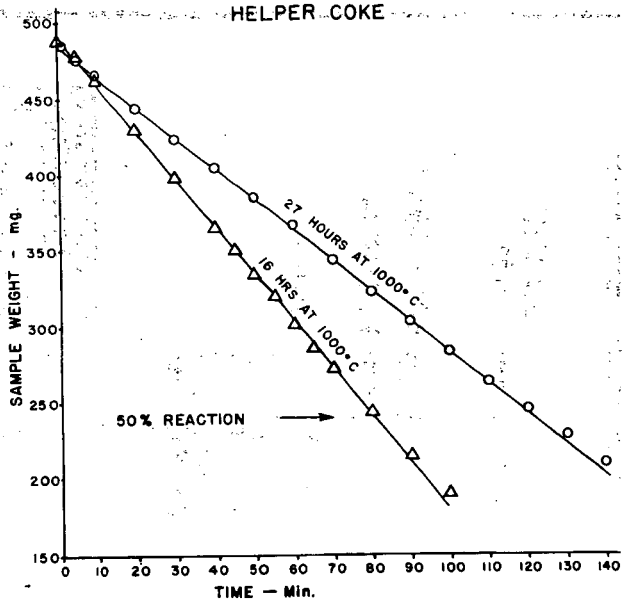


FIG. 2

REACTION OF HELPER COKE SOAKED AT 1000°C

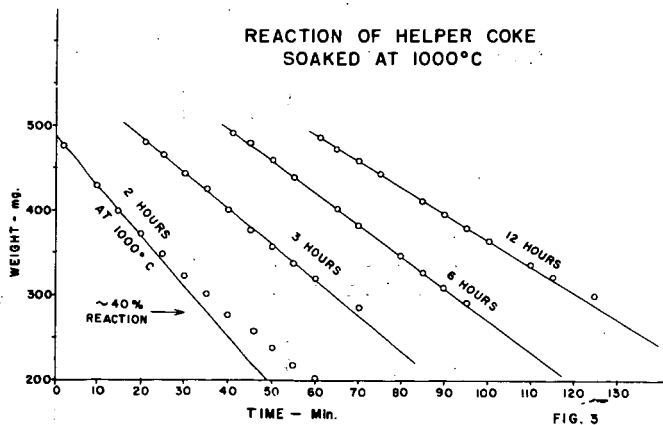
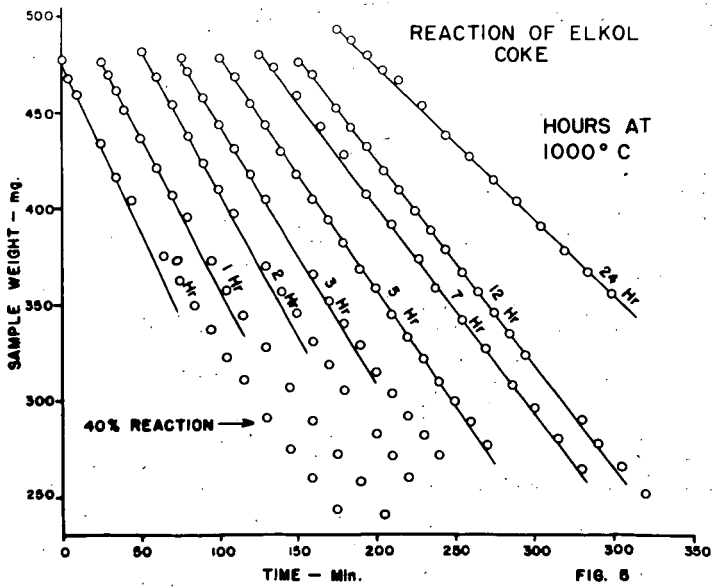
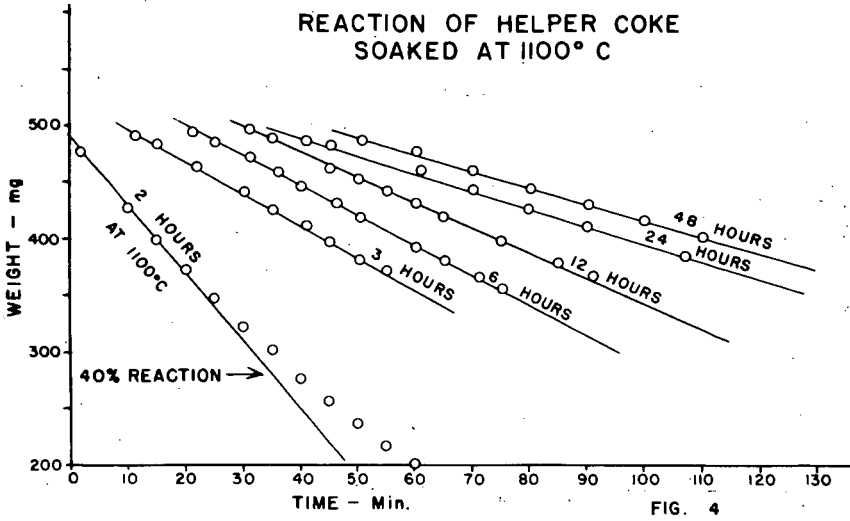


FIG. 3



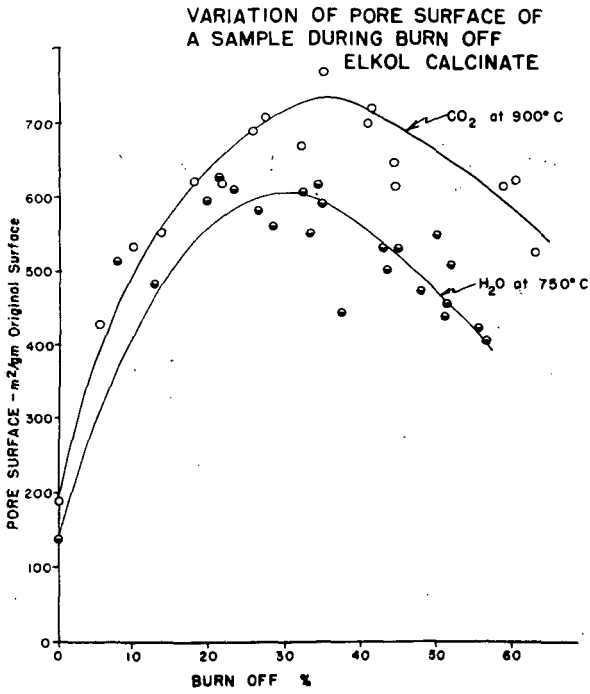


FIG. 6

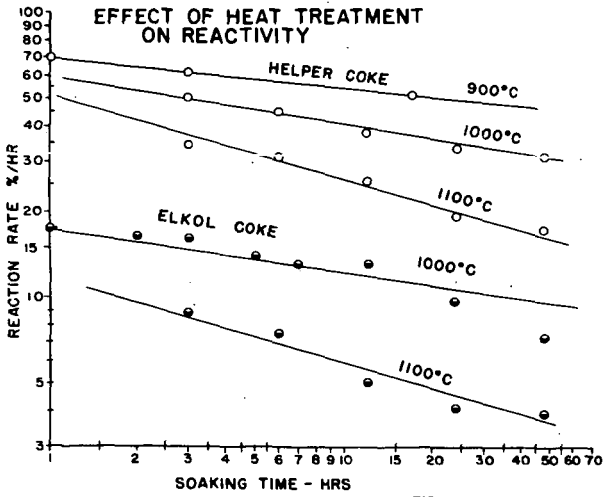


FIG. 7

EFFECT OF INHIBITORS ON FLAMMABILITY OF HEPTANE-AIR MIXTURES

H. Landesman and J. E. Basinski

National Engineering Science Company, Pasadena, Calif.

A large scale investigation of the effect of inhibitors on flammabilities of heptane-air mixtures has been reported by workers at Purdue University (2)(3). The technique involves measuring upward flame propagation at various n-heptane inhibitor-air percentages in a standard 4 ft. long, 2 in. diameter tube and plotting the percentages of extinguishant versus heptane percentages where mixtures are nonflammable. A curve such as shown in Fig. 1 is obtained.

With better inhibitors than that shown in Fig. 1, a peak in the flammability curve will be obtained at a lower percentage of inhibitor than the 6 mol. percent of Fig. 1. This peak percentage may be translated to weight percentages of inhibitor producing nonflammability of heptane-air mixtures and comparisons on a weight basis also can be obtained. These data have been found to follow fairly closely the extinguishment capability of the materials on actual test heptane or gasoline fires (3), though there is controversy over the extrapolation of data to potential fire extinguishing performance (4).

It was necessary to obtain a pre-fire test screening of extinguishants for hydrocarbon fires which would be stable at 550° F and have low vapor pressures at that temperature. This screening was accomplished by means of the combustion tube apparatus mentioned before. Since high concentrations of low vapor pressure inhibitors could not be maintained in the vapor phase with heptane-air mixtures in a conventional ambient temperature flammability limit combustion tube (5), it was necessary to design a heated combustion tube in which the flame propagation could still be observed. Visibility was necessary for evaluation of the inhibitory effects of the candidate extinguishant.

Experiments were carried out at sub-atmospheric pressures to prevent explosions or excessive pressures in the tube. Relative inhibitory effects have been found to be essentially independent of pressures down to about 200 mm (2).

The system is diagrammed in Fig. 2 and photographs are shown in Figs. 3 and 4. The gas containing sections of the apparatus are heated to 200°C to prevent condensation of the inhibitor. The glass combustion tube is heated by a baked on transparent conductive coating, while the metal inlet system and the pressure gauge are heated by electrical tapes.

The lower end of the combustion tube is closed by a metal flange, which is joined to the tube by a kovar-glass seal. The removable half of the flange has a glass feed-through insulator for the tungsten ignition wire (Fig. 4). This entire flange assembly and lower end of the tube is submerged in the 200°C silicone oil bath to insure the gases reaching a uniform temperature.

Partial pressures of the inhibitor and the heptane are measured directly with a Kern-Springham glass spiral manometer with attached mirror. Rotation of the spiral deflects the mirror and the deflection is measured on the scale.

The spiral deflection was calibrated to read pressures up to 50 mm against an external mercury manometer which was read with a cathetometer. Total pressure of the combined inhibitor-heptane-air mixtures was 300 mm.

For the larger air pressures, the manometer is used as a null indicator. The desired air pressure is introduced to the outside of the glass spiral, then balanced with pre-heated air on the system side. The gases are mixed by a sliding perforated disc, which is driven by an external magnet. After twenty minutes of mixing, the disc was brought to the top of the tube and the mixture sparked. If ignition, as evidenced by flame propagation to the top of the tube, did not occur, mixing was continued another five minutes and the mixture sparked again. It was found that the rich limit for heptane-air increased to 8.75 percent heptane at 203°C and 300 mm total pressure compared to 6.9 percent at approximately ambient temperature and 300 mm pressure (2). The lean limit did not change. A few comparison points were made in this work at 203°C with the same inhibitors used in the Purdue work at ambient temperatures. It was found that peak percentages for sym-dibromotetrafluoroethane and for trifluorobromomethane increased about 10 - 12 percent with the temperature increase. However, since experimental conditions, including mixing times and methods of mixing, are considerably different, the comparison has little meaning. It was found during this work that changes in these variables led to large differences in observed flammability.

In Figs. 5, 6, 7 and 8 are shown flammability plots for the inhibitors evaluated. The curves exhibit a variety of shapes and peaks occurring at various heptane-air-inhibitor ratios. The significance of this is not known. The peaks of the curves are of interest since these represent a comparison of the individual molecules' effectiveness as flame inhibitors. In Table I are presented data obtained on peak inhibition percentages and the weight this volume percentage represents in 100 liters of a heptane-inhibitor-air mixture. These data are taken from peaks of the curves previously shown.

The Purdue University work previously referenced contained a study of the effectiveness of 56 compounds as flame inhibitors, in a combustion tube at room temperature. This study includes many halogenated hydrocarbons, however, since their tube was not heated, they were unable to test the less volatile materials. Two major correlations emerge from their work, the first is a confirmation of work of earlier investigators who found that hydrocarbons containing iodine are better extinguishants than those containing bromine, which in turn, are better than the aliphatic chlorides. The Purdue group also found that hydrocarbon compounds containing only fluorine were very poor extinguishants. The second major correlation was the observation that as the molecular weight increases the extinguishing ability also increases, i.e., the peak percentage decreases. This relation, however, is not invariable and it is not possible to determine the extinguishing ability of a molecule from its molecular weight alone.

This study was carried out at a temperature of 203°C, thus, it was possible to determine the peak percentages of some higher molecular weight halogenated hydrocarbons. Figure No. 9 is a plot of the peak percentages from all the Purdue data plus those determined in this work as a function of molecular weight. The situation is quite complex, however, the chlorine containing compounds appear to form a rough series.

The general curvature of this line suggests that a straight line might occur if peak percentage were plotted against the inverse molecular weight. As can be seen from Figs. 10 - 14, this is the case. For a given series of halogenated hydrocarbons, the general trend is quite well marked, despite the wide variation in structures. There are two possible explanations that might clarify this relationship between peak percentage and inverse molecular weight. The first would be a purely physical process in which the extinguishant molecule acts as a "third body" to promote free radical recombinations. The alternate possibility would be to reason that the inverse molecular weight was related to some chemical property, such as bond energy, which was the actual cause of the effectiveness of the extinguishant. At the moment, we are investigating various parameters in an attempt to discover a rational correlation and explanation of the relation of extinguishant ability to the physical properties and chemical structures of the halogenated hydrocarbons.

References

1. This work was supported by the Federal Aviation Agency under U.S. Air Force Aeronautical Systems Division Administration on Contract AF33(657)-8937.
2. McBee, E. T., et al, AT1114, 903 Report on USA Contract W-44-009. ENG-507.
3. Malcolm, James E., National Fire Protection Quarterly, October 1954.
4. Engibous, E. L. and Torkelson, T. R., WADC-TR-59-463, p. 9.
5. Coward, H. F. and Jones, G. W., Bureau of Mines, Bulletin 503.

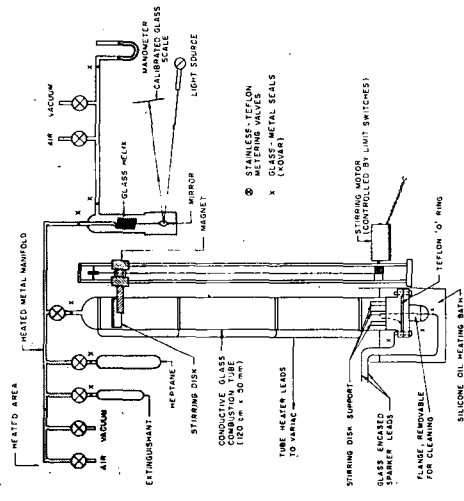


FIGURE 2
COMBUSTION TUBE FOR FLAMMABILITY LIMIT STUDIES (DIAGRAM)

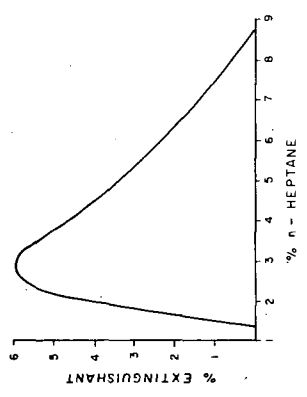


FIGURE 1

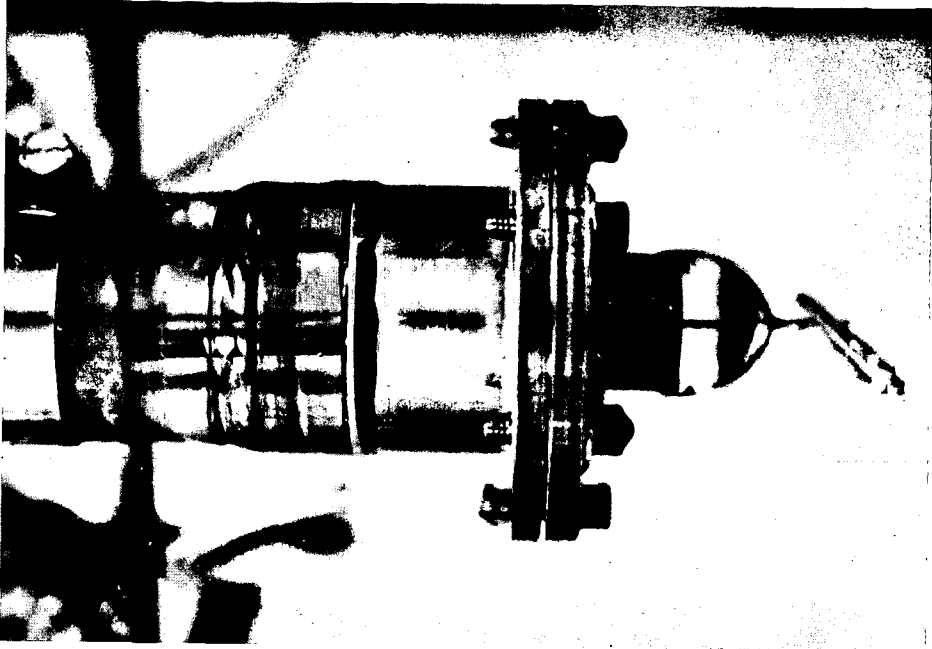


FIGURE 4 FLANGE DETAIL

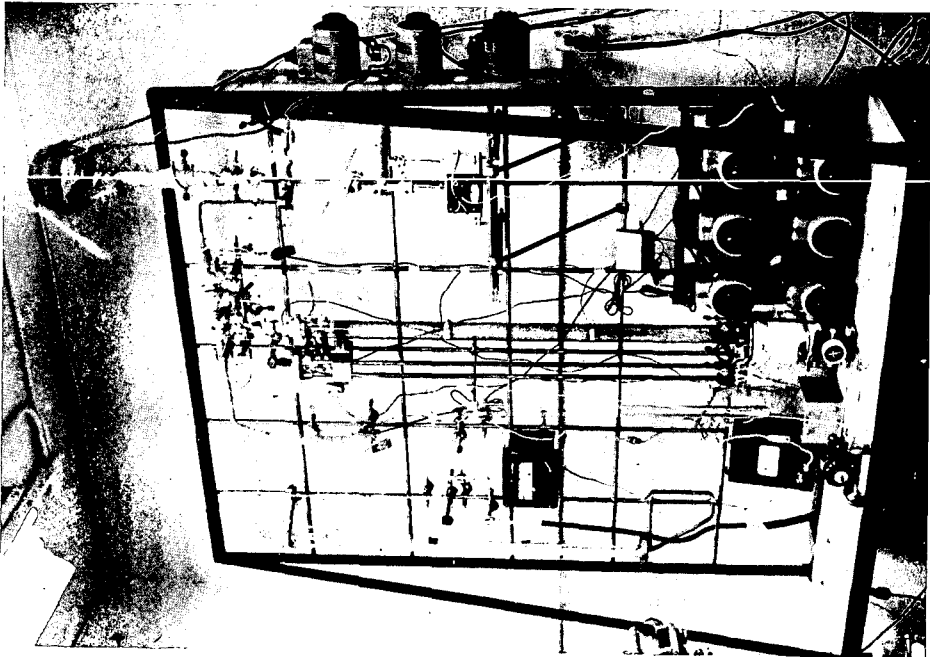


FIGURE 3 COMBUSTION TUBE

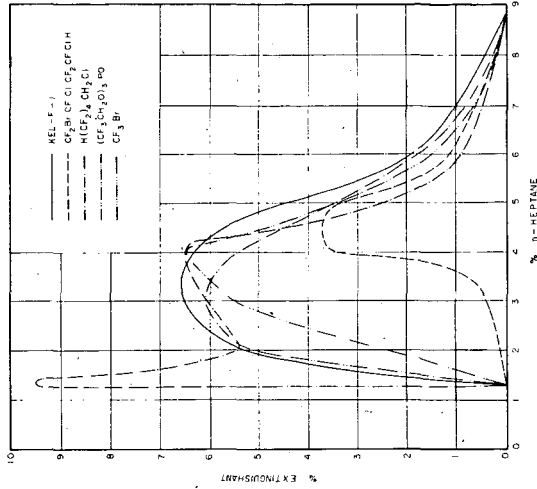


FIGURE 6
EFFECT OF CANDIDATE EXTINGUISHANTS ON FLAMMABILITY
OF n - HEPTANE - AIR MIXTURES

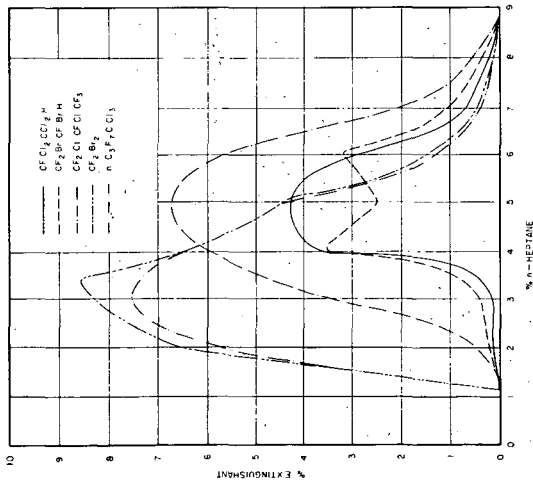


FIGURE 5
EFFECT OF CANDIDATE EXTINGUISHANTS ON FLAMMABILITY
OF n - HEPTANE - AIR MIXTURES

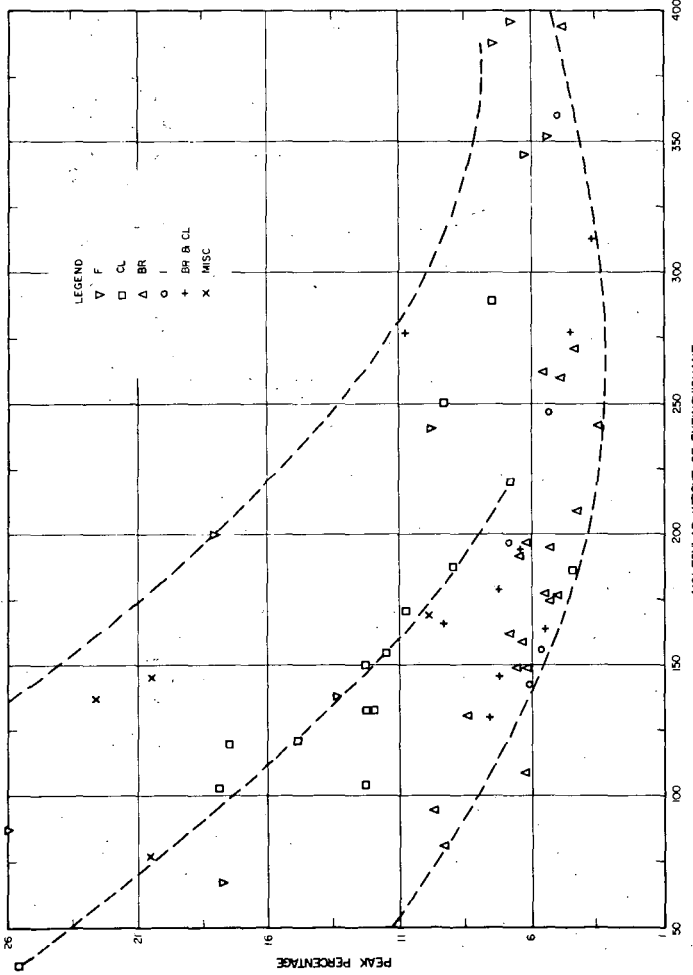


FIGURE 9
PEAK PERCENTAGE OF EXTINGUISHANT TO RENDER HEPTANE-AIR MIXTURE NON-FLAMMABLE AS A FUNCTION OF EXTINGUISHANT MOLECULAR WEIGHT

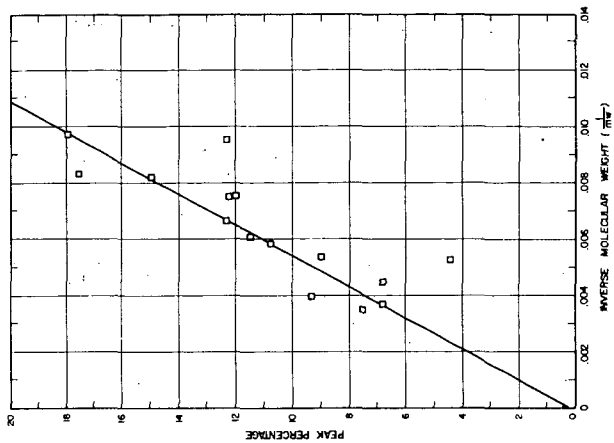


FIGURE 11
PEAK PERCENTAGE OF CHLORINE CONTAINING EXTINGUISHANTS AS A FUNCTION OF $1/MW$

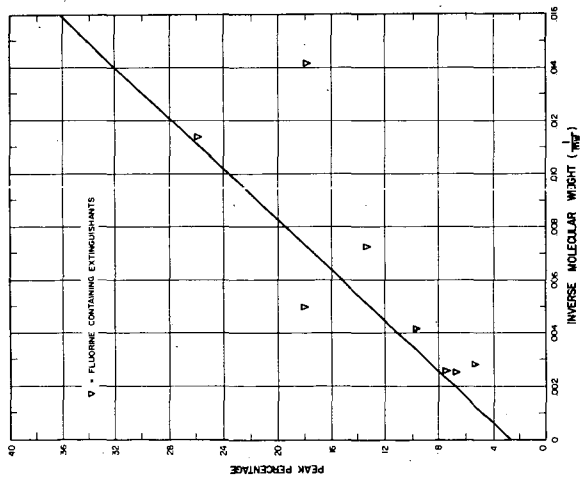


FIGURE 10
PEAK PERCENTAGE OF FLUORINE CONTAINING COMPOUNDS AS A FUNCTION OF INVERSE MOLECULAR WEIGHT

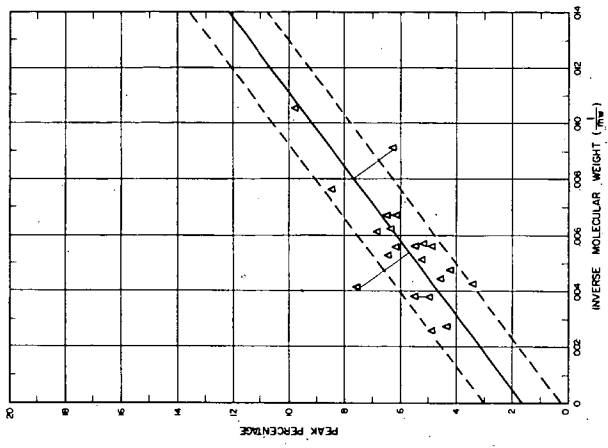


FIGURE 13
PEAK PERCENTAGE OF BROMINE CONTAINING EXTINGUISHANTS AS A FUNCTION OF $1/MW$

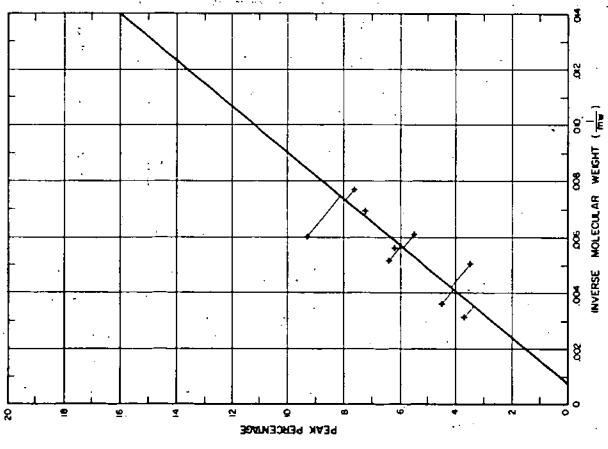


FIGURE 12
PEAK PERCENTAGES OF COMPOUNDS CONTAINING BOTH CHLORINE AND BROMINE AS A FUNCTION OF INVERSE MOLECULAR WEIGHT

TABLE I
EFFECT OF INHIBITORS ON HEPTANE-AIR FLAMMABILITY

Total Pressure 300 mm, Temperature 398° F

MW	Peak %	Wt. at Peak %	Bank Wgt. Basis	Bank Vol. Basis
197.5	3.5	30.7	1	2
186	4.4	36.6	2	4
242	3.4	36.8	3	1
164	5.5	40.3	4	9
149	6.5	43.2	5	13
224	4.5	45.0	6	5
195	5.2	45.3	7	8
314	3.7	51.8	8	3
276.5	4.5	55.5	9	6
260	5.5	65.8	10	10
221	6.8	67	11	14
270.5	6.8	78.5	12	15
150.5	12.3	82.6	13	20
395	4.75	81.6	14	7
287.5	7.5	96.5	15	16
344	6.3	96.7	16	11
295	7.5	99.0	17	37
250.5	9.3	104.2	18	19
500 Av.	6.5	145.0	19	12
671	7.5	219.0	20	18

CF₃CHBrCl
CF₃CHCl₂
CF₂BrCHBrF
CHBrCl
CHBrF
CH₂BrCF₂
CHF₂CF₂Br
CF₂CF₂CF₂CHClF
CF₂CF₂CF₂CHClF
CF₂CF₂CF₂
CCl₂CF₂CF₂
CHF₂CF₂CH₂Cl
CHF₂(CF₂)₂CH₂Br
CF₂CF₂CF₂CCl₂
(CF₂CH₂)₂PO
CHF₂(CF₂)₂CH₂Br
CHF₂(CF₂)₂CH₂Cl
KEL-F-1 fluoro-
fluoroolefin polymer
(CF₃CF₂)_n

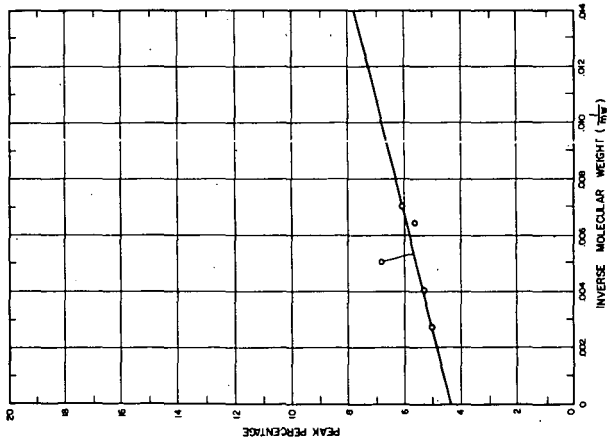


FIGURE 14
PEAK PERCENTAGE OF IODINE CONTAINING EXTINGUISHANTS AS A FUNCTION OF 1 / MW

Ignition Characteristics of Colorado Oil Shale

V. Dean Allred and L. S. Merrill, Jr.

Marathon Oil Company, Littleton, Colorado

Introduction

Spontaneous ignition is usually characterized by an abrupt (exponential) increase in temperature and results when the rate of heat production in exothermic reaction exceeds the rate of heat dissipation to the surrounding media. Ordinarily the term spontaneous ignition temperature is applied to those systems being oxidized by air. However, in this paper the term applies to systems using oxygen enriched or partially depleted gas streams.

In a practical application it is important to know the ignition characteristics of oil shale in developing an understanding of processes for recovering oil from oil shales. This is particularly true when using the countercurrent or reverse combustion in situ recovery or the parallel flow retorting process (1, 2).

The countercurrent combustion process is one in which the combustion or oxidation zone moves against the flow of the injected gas stream. Figure 1 shows a schematic representation of such a process. To be practical, the combustion zone must progressively move toward the source of the oxidant injection at such a rate that only a minimum amount of fuel is consumed and the useful products produced in an oxygen free atmosphere. The process is somewhat unconventional but has been demonstrated in the laboratory as a means of producing oil from oil shale.

One way of explaining why the process works is as follows: As ignition of a given particle takes place, it is accompanied by an exponential temperature rise which in turn causes a rapid increase in combustion (oxidation) rate. This effectively removes the oxygen from the surrounding gas stream, so no further oxidation takes place at this point. However, heat has been transferred to the surrounding particles as well as the gas stream. One effect is that particles immediately upstream are continuously being heated to their ignition temperature and the process repeats itself with the combustion zone effectively progressing against the gas flow. Another effect is that the oxygen has been efficiently removed from the gas downstream from the combustion zone. This provides an inert hot gas in which the hydrocarbon components are effectively distilled from the solids.

Experimental

In this investigation the ignition temperatures were determined in a flow-type system so that conditions would be somewhat comparable to the retorting process. The experimental arrangement is given in Figure 2.

The basic unit of equipment was a small Inconel block furnace containing two one-half inch sample holes. One hole contained the sample and the other was filled with an inert reference material. Alternate junctions of twelve chromel-alumel thermocouples were located in the two holes to form a sensitive thermopile detector.

Since ignition is characterized by a rapid temperature rise, the differential thermopile was used in most experiments to detect the temperature at which combustion

occurred. However, advantage was also taken of the fact that ignition is also accompanied by the simultaneous release of carbon dioxide. In the latter case, the gas stream was continually monitored as a function of temperature with a differential thermal conductivity cell. Both techniques proved equally effective.

Determinations were made in air and in gas mixtures of oxygen and nitrogen over a pressure range from atmospheric to 1000 psig. The gas mixtures contained six, thirteen, twenty-one, and fifty-five percent by volume of oxygen.

In a typical experiment, about two grams of -40 to 60 mesh oil shale was placed in the sample hole. A similar sized sample of previously pyrolyzed oil shale was placed in the reference cell. The oxidant containing gas passed at the same rate through the shale and the reference material at the pressure of the experiment. The block was heated at a uniform rate of about 40°F/minute. Temperature and differential temperature were recorded by use of either a two-pen or an x-y recorder. In the alternate detection system the off-gas was taken from the cells, passed through drying tubes to remove water vapor, and then to the reference and sample sides, respectively, of a thermal conductivity detector. This signal was then continuously recorded as a function of the sample temperature.

Experimental Results

Ignition temperatures as a function of oxygen partial pressure for data covering several oxygen concentrations in the gas stream are tabulated in Table I and shown in Figure 3. (Note: These data are plotted with the square root of the oxygen partial pressure as a coordinate so that the scale could be expanded on the low pressure end and still extrapolated to zero. Plotting the square root has no other significance). From the curve shown in Figure 3 it is readily observed that the ignition temperature is relatively independent of total pressure, but strongly dependent on the oxygen concentration.

Other data have shown that lower rates of supplying the oxygen has little or no effect on the ignition temperature as long as excess oxygen is present for the combustion reaction.

One interesting set of data are shown in Figure 4. Of particular interest are the characteristics of the ignition temperatures at pressures below 100 psig where two temperature peaks were noted. The first peak showed a temperature rise but did not result in ignition.

These same data are plotted as a function of oxygen partial pressure in Figure 5, which shows the nature of the transition region clearly. It is thought that this transition region is associated with the well known "cool flame" oxidation phenomena observed for ignition of many hydrocarbons as a function of pressure. For example, Figure 6 shows these oil shale data, together with ignition curves, for n-octane, i-octane, and propane (3, 4). Naturally one would not expect the data to coincide with these particular hydrocarbons, but the similarity of the shape of the curves and the temperature range is striking. One possible interpretation of this behavior is that the shale ignition is associated with gas phase combustion of hydrocarbons being distilled out of the oil shale.

Discussion

The question arises why oil shales ignite at such low temperatures when destructive distillation of the shale oil does not occur until temperatures in excess of 700°F are reached.

This question can possibly be answered by considering the fact that Colorado oil shale has from one to three percent by weight (about ten percent of total

TABLE I

<u>Gas Composition</u> <u>Volume %</u>	<u>Total Pressure</u> <u>(psi)</u>	<u>*Oxygen Partial</u> <u>Pressure (psi)</u>	<u>Ignition</u> <u>Temperature (°F)</u>
(Air)	125	24	450
(21% O ₂)	162	34	435
	212	44	435
	587	123	385
	954	203	365
	22.2	4.7	545
	32.2	6.8	540
	32.2	6.8	535
	52.2	11.0	500
	72.2	15.1	475
	26.2	5.5	530
	92.2	19.4	465
	112.0	23.6	455
	212.0	44.5	425
<hr/>			
(55% O ₂)	22.2	12.2	455
(45% N ₂)	112	61.7	400
	210	116	375
	512	281	354
	812	446	340
<hr/>			
(13% O ₂)	22.2	2.9	580
(87% N ₂)	44.2	5.7	560
	60.2	7.8	500
	110	14.4	495
	167	21.8	453
	594	77.3	395
<hr/>			
(6% O ₂)	22.2	1.3	586
(94% N ₂)	39.2	2.4	565
	62.2	3.7	535
	112	6.7	506
	277	16.6	435
	860	51.6	405

*Data taken at gas flow rate of 1350 standard cubic feet per square foot of cross sectional area per hour.

organic matter) of benzene soluble components in it. As shown in Figure 7, about the same weight fraction of oil shale is volatile between 360°F and 700°F when analyzed by thermogravimetric (TGA) techniques. These data indicate that volatiles start being evolved in an appreciable amount at about 360°F, which was about the same as the lowest self ignition temperature observed. Further, this preliminary evolution reaches a maximum at about 600°F, which is about the normal ignition temperature in air at atmospheric pressure.

Based on these data, it seems very likely that ignition is associated with the evolution of hydrocarbon vapors from the oil shale in the temperature range 360°-700°F.

Summary

The self ignition temperature of Colorado oil shale has been determined to vary with oxygen concentration from about 630°F at atmospheric conditions to 360°F at high (about 500 psi) oxygen partial pressure.

The ignition temperature is shown to correspond closely to temperature range during which organic vapors evolve prior to the onset of destructive distillation of the kerogen in the shale.

Literature Cited

1. Allred, V. D., and Nielson, G. I., Countercurrent Combustion - A Process for Retorting Oil Shale. Preprint No. 9, AIChE 48th National Meeting, Denver, Colorado.
2. Allred, V. D., U. S. Patent 3,001,775 (September 26, 1961) assigned to Marathon Oil Company.
3. Affens, W. A., Johnson, J. E., and Carhart, H. W., Ignition Studies Part V., NRL Report 5437 (January 27, 1960).
4. Maccormac, M., and Townsend, D. T. A., The Spontaneous Ignition Under Pressure of Typical Knocking and No-Knocking Fuels: Heptane, Octane, Iso-octane, etc. J. Chem. Soc. 143 (1940).

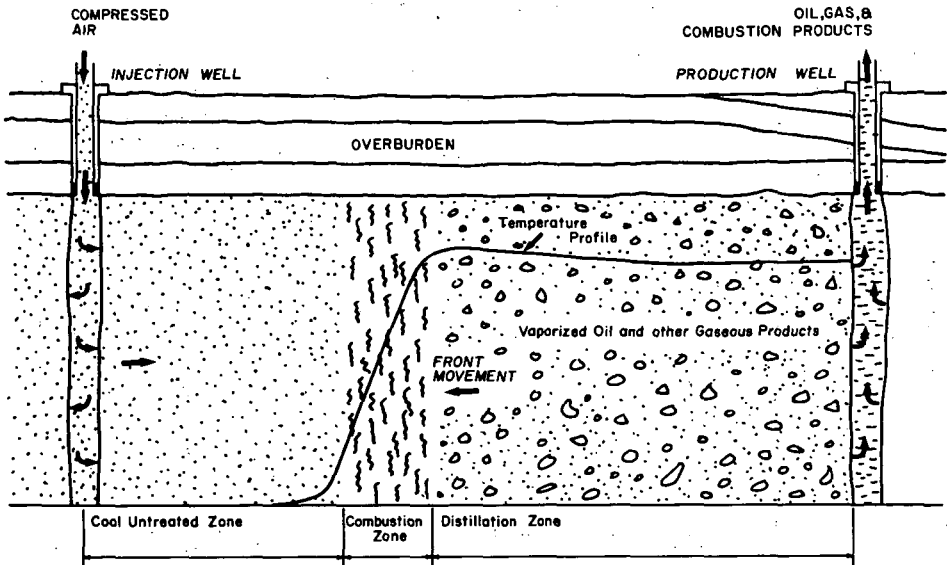


Figure 1. The Countercurrent Combustion In Situ Process for Recovering Hydrocarbons.

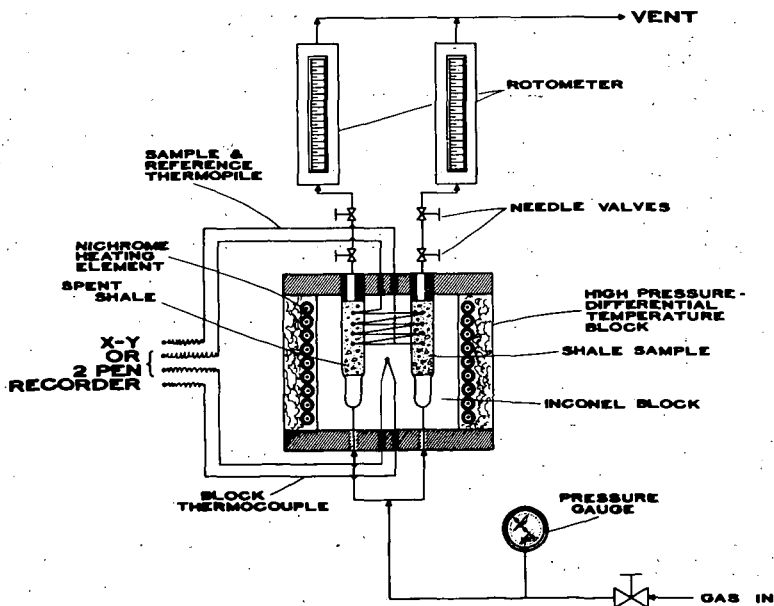


Figure 2. High Pressure Differential Analysis Equipment for Determining Spontaneous Ignition Temperature of Oil Shale.

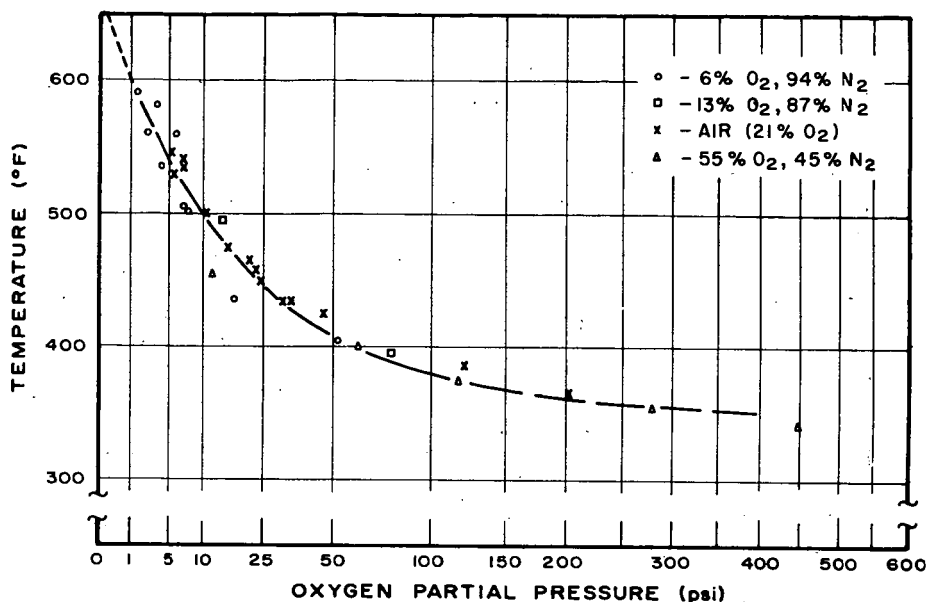


Figure 3. Ignition Temperature of Colorado Oil Shale as a Function of Oxygen Partial Pressure.

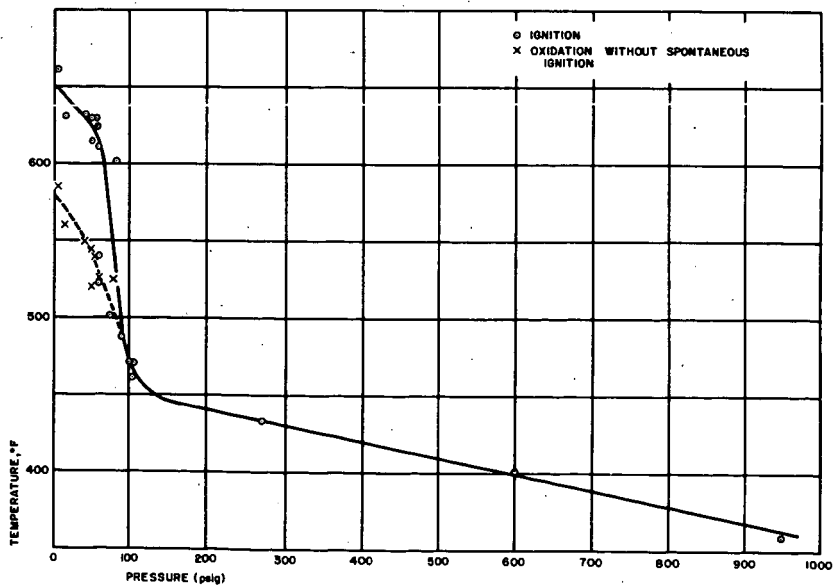


Figure 4. Spontaneous Ignition Temperature of Colorado Oil Shale as a Function of Pressure.

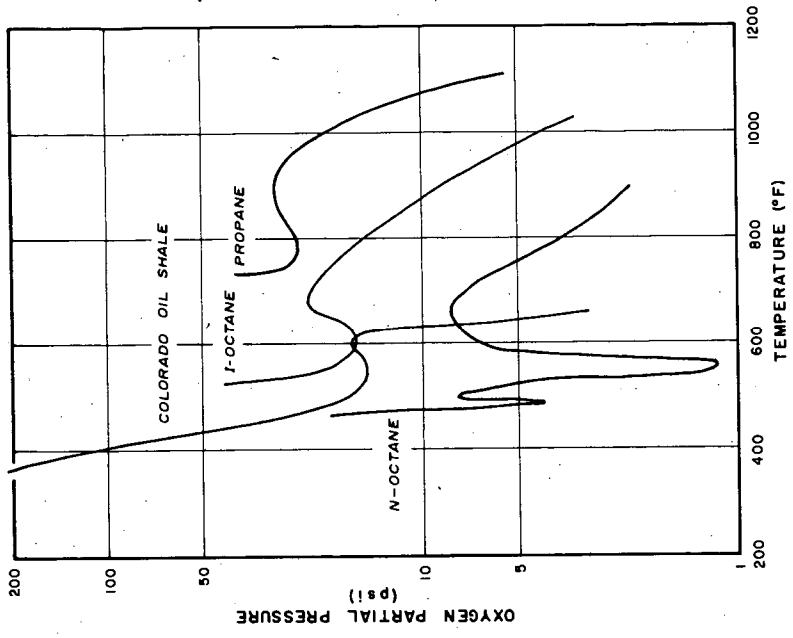


Figure 6. Spontaneous Ignition Curves for Selected Hydrocarbons.

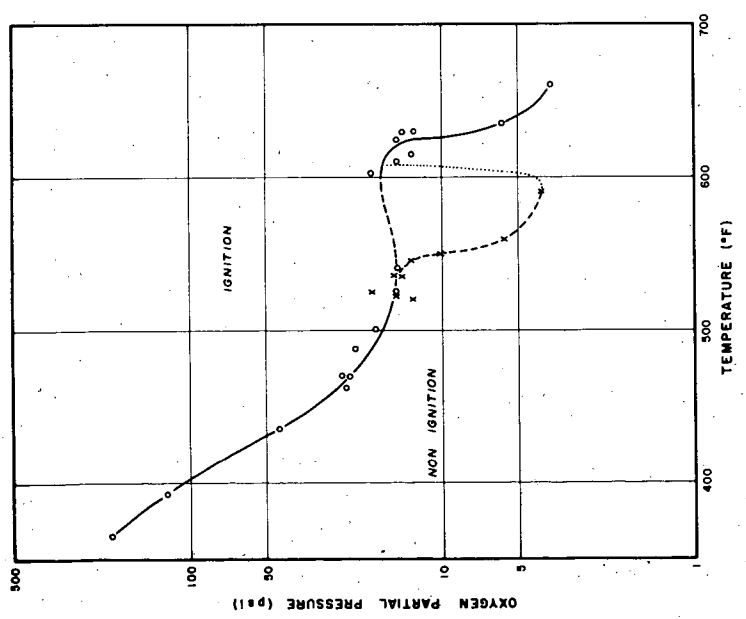


Figure 5. Spontaneous Ignition Curve for Colorado Oil Shale.

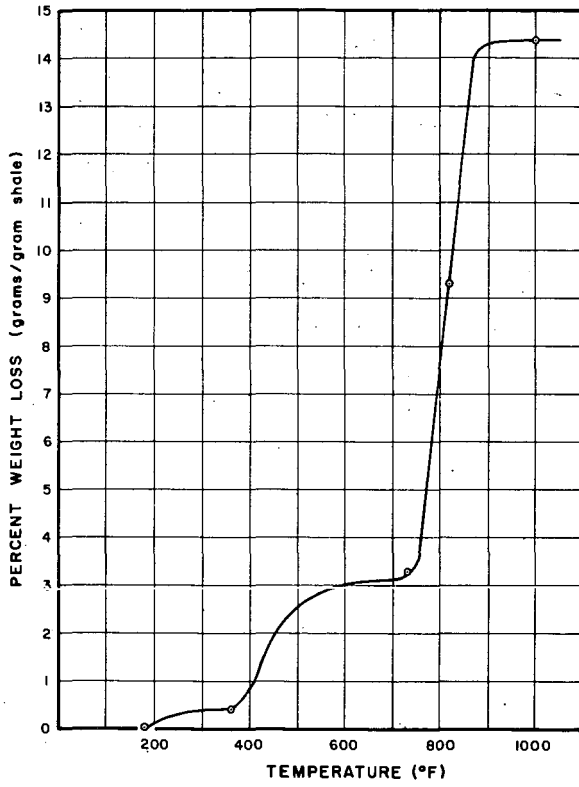


Figure 7. TGA of Colorado Oil Shale.

Production of Alcohols from Olefins in Low Temperature Coal Tars

Bernard D. Blaustein, Sol J. Metlin, and Irving Wender

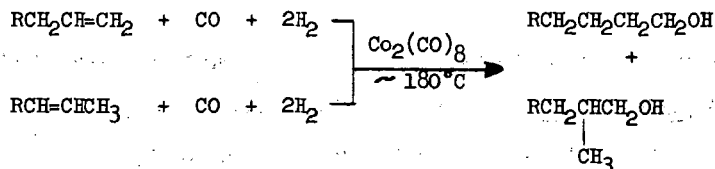
Pittsburgh Coal Research Center, Bureau of Mines
U. S. Department of the Interior
4800 Forbes Avenue, Pittsburgh 13, Pennsylvania

ABSTRACT

Olefins constitute as much as one-half the neutral oil obtained by low-temperature carbonization of low-rank coals. It is difficult to separate these olefins from other materials in the tar fractions. However, without a prior separation, a large fraction of these olefins can be converted to mixtures of primary alcohols by hydroformylation with $H_2 + CO$ in the presence of dicobalt octacarbonyl as a catalyst (oxo reaction). Several neutral oils were so treated and the alcohols separated via their borate esters. The highest yields of alcohols (25 percent by weight of starting material) were obtained from the neutral oil of a lignite tar. The carbon number distribution of the alcohols was determined by mass-spectrometric analysis of the trimethylsilyl ethers. C_9 - to C_{27} -alcohols were produced; an unusually high concentration of C_{20} -alcohols appeared in the products from lower rank coals. Nuclear magnetic resonance spectra of the alcohol mixtures showed that an "average" molecule contains from 1 to 3 branched methyl groups. By using $C^{14}O$, and assuming that each olefin will react with one CO , the percentage of olefins originally in the tar can be determined from the radioactivity of the product. An advantage of this analytical method is that no separation of the olefins, or their oxo product, need be made. By this procedure, the neutral oil from the lignite tar was shown to contain about 50 percent olefins.

INTRODUCTION

The high olefinic content of tars derived from low temperature carbonization of lower rank coals is of interest as a source of commercially valuable chemicals. However, there is no good way of separating these olefins from the other materials present in the tar fractions. The oxo (or hydroformylation) reaction offers a promising way to convert the olefins in the tar, without prior separation, to alcohols that are of potential commercial value as detergent and plasticizer intermediates. The oxo synthesis (1) is the reaction of an olefin with $H_2 + CO$ (synthesis gas) in the presence of dicobalt octacarbonyl, $Co_2(CO)_8$, as the catalyst to yield a mixture of primary alcohols.



The reaction takes place predominantly at the terminal double bond.

The advantages of using this reaction to convert olefins to useful products are (a) the olefins need not be separated from the tar fractions to undergo reaction, (b) the reaction is not poisoned by sulfur compounds or any of the other substances in low-temperature tar, (c) conversion of the olefins is high, (d) during the oxo reaction, any internal olefinic bonds migrate to the terminal position so that all olefins react as if they were alpha olefins; all the olefins in the tar, terminal and internal, are thus utilized to make alcohols, and (e) the oxo reaction is quite versatile and can be successfully carried out under a wide range of conditions: gas pressures of 50-400 atm, and reaction temperatures of 50-200°C.; $\text{Co}_2(\text{CO})_8$ can be used either in the preformed state, or can be formed during the reaction from a variety of cobalt salts.

EXPERIMENTAL

Samples of Rockdale lignite tar were obtained from the Texas Power and Light Company. They had separated the whole lignite tar into "methanol solubles" and "hexane solubles." The hexane solubles were further separated by distillation into two fractions, the hexane solubles foreruns (HSF) and the hexane solubles distillate (HSD). The total hexane solubles constitute 66 percent of the primary tar; the HSF 7 percent, the HSD 46 percent, and the residue from the distillation of the hexane solubles 13 percent. About 98 percent of the HSF boils below 235°C., and 89 percent of the HSD boils up to 355°C. The composition of these fractions is given in table 1.

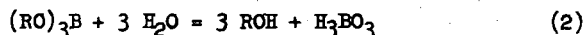
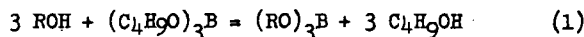
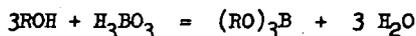
Both fractions contain approximately 50 percent olefins, of which about half are alpha olefins (2-4). Phenolic compounds and other constituents are also present in both fractions. Since these phenols would interfere with our analytical procedure for determining alcohol yield, they were removed by chromatographing the fractions on alumina with petroleum ether as the eluting solvent. About 20 percent by weight of the starting material was removed in this way during the preparation of a "phenol-free" lignite tar fraction.

TABLE I.-Approximate composition of low-temperature tar fractions, volume percent

Type of constituent	Hexane	Hexane	Nugget tar distillate	Kentucky high-splint tar distillate
	solubles foreruns	solubles distillate		
	Rockdale lignite tar			
Caustic solubles	6-8	10-15	44	31
Acid solubles	2-4	1-3	3	7
Neutral oil	88-92	80-90	53	62
Paraffins	13-15	15-20	22	34
Olefins	40-55	40-50	20	21
Alpha-olefins	17-20	17-20		
Aromatics	30-47	35-45	37	45
Oxygenates			21	

Nugget tar, formed by the low-temperature carbonization of a hvcb-suba Wyoming coal, was also investigated. A sample of this tar was distilled under vacuum to 170°C/3mm (est. bp 320°C/760mm). The distillate, including a small amount of water phase, amounted to 42.1 percent of the whole tar. Repeated chromatography finally yielded a phenol-free neutral oil amounting to 37.9 percent of the distillate. A neutral oil derived from the low-temperature carbonization of a Kentucky hvab (high splint) coal was chromatographed on alumina to eliminate the phenols shown to be present by infrared spectral analysis. Recovery of phenol-free neutral oil was 86.8 percent.

The alcohols were separated from the oxo products by conversion to their borate esters (5-8). The borate esters formed from the alcohols are sufficiently high-boiling that the non-esterified material can be distilled away from the esters. The esters are hydrolyzed to regenerate the alcohols, which are then separated and vacuum distilled, resulting in an alcohol fraction of high purity.



In a typical run, 50 grams of chromatographed (phenol-free) HSF, 4 grams of $\text{CO}_2(\text{CO})_8$ and 3500 psi 1:1 synthesis gas were charged into a rocking Aminco autoclave, heated to 180-190°C. and kept there for five hours. The product was treated with tri-n-butylborate (equation 1), the non-esterified material was distilled off, the borate esters were hydrolyzed

(equation 2), and the alcohols were vacuum distilled. The product was an almost water-white alcohol fraction in 25 percent yield, based on the weight of starting material. The alcohol content was confirmed by infrared spectral analysis, the only impurity detected being a small amount of a carbonyl compound. To determine the carbon number distribution of the alcohols formed, the trimethylsilyl ethers of the alcohols were analyzed by mass spectrometry (9). The results are shown in figure 1.

The chromatographed (phenol-free) HSD was subjected to the same reactions and subsequent procedures for alcohol recovery. The alcohol yield was also 25 percent by weight of the starting material; the carbon number distribution data is given in figure 2. The phenol-free neutral oil from the Nugget tar distillate was subjected to the oxo reaction and the same alcohol recovery procedures as those previously described for the Rockdale tar. An alcohol yield of 13 percent was realized. The alcohols were converted to their trimethylsilyl ethers and analyzed by mass spectrometric analysis. The results are shown in figure 3. The phenol-free neutral oil from the Kentucky hvab coal was reacted under oxo conditions. The subsequent recovery of alcohol was 7.5 percent. The product, water-white in color, was converted to trimethylsilyl ethers and submitted for mass spectrometric analysis. The results are shown in figure 4.

NMR spectra were obtained on all the alcohol mixtures produced from the tar fractions. These results will be considered in the Discussion section of this paper.

Under oxo conditions, it can be assumed that each molecule of olefin will react with one molecule of CO. Further reaction under oxo conditions will produce alcohols, aldehydes, esters, and other oxygenated products. If $C^{14}O$ is incorporated into the synthesis gas, the product will be radioactive. A determination of the amount of radioactivity in the product can then be used to calculate the concentration of olefins present originally in the tar fraction. Several runs of this type were made, both on known mixtures, and on the low-temperature tar fractions. The results obtained are discussed below.

RESULTS AND DISCUSSION

Carbon Number Distribution of Alcohols Produced

Figure 1 shows the distribution of the alcohols produced from the HSF fraction of the lignite tar. The carbon number range shown is C_{10} - C_{15} , the maximum concentration is at C_{12} , and the average carbon number is 12.2. Not shown on the graph are minor concentrations of C_9 and C_{16} - C_{20} alcohols. This mixture is composed of alcohols of the carbon number

range now used for plasticizer and detergent production. A higher boiling fraction of these alcohols ranged from C_9 to C_{24} , with an average carbon number of 16.2. Figure 2 shows the distribution of the alcohols produced from the HSD fraction of the lignite tar. The carbon number range shown is C_{13} - C_{22} , the largest percentage is at C_{20} , and the average carbon number is 17.8. There are also traces of C_{11} - C_{12} and C_{23} - C_{27} alcohols.

Figure 3 shows the distribution of alcohols produced from the neutral oil from the Nugget tar distillate. The carbon numbers range from C_{11} - C_{23} , the largest concentration is at C_{15} , and the average carbon number is 16.3. Trace amounts, not shown, are also present at C_{24} and C_{25} . Figure 4 shows the distribution of the higher boiling alcohols produced from the neutral oil from the Kentucky hvab coal. The carbon numbers range from C_{13} - C_{23} , the greatest concentrations are at C_{16} and C_{17} , and the average carbon number is 17.2. Trace amounts, not shown, were also present at C_{24} . A lower boiling fraction of these alcohols ranged from C_{10} to C_{22} , with an average carbon number of 14.1.

In the alcohol mixtures produced from the lower rank lignite and hvab-suba coals, there are anomalously high concentrations of C_{20} alcohols. (See figures 2 and 3.) This did not appear in the alcohols from the hvab coal (figure 4). Gas-chromatographic methods, and other separation techniques, will be used to obtain highly concentrated samples of either the C_{20} alcohols and/or their precursors, the C_{19} olefins from the lignite tar. If identification of either the alcohols or olefins can be made, it may point out interesting differences between the low-temperature carbonization tars produced from low and medium rank coals. It is conceivable that the C_{19} olefin present in such high concentration in the tars from the lower rank coals is some isomer of pristene (2,6,10,14-tetramethylpentadecene), since the saturated paraffin, pristane, recently has been isolated from a low-temperature brown coal tar (10), and was shown to be present in abnormally high concentrations in two petroleum (11).

NMR Spectra of Alcohol Mixtures

The NMR spectra of these alcohol mixtures were run on a Varian HR-60 instrument. Data were obtained for the number of H atoms on the C atom bonded to the OH group (that is, if the alcohol is a primary alcohol), and the number of H atoms present in methyl groups. This latter quantity gives a measure of the branching of the carbon chain.

For the HSF alcohols, there were 1.8 H atoms on C bonded to OH, and 1.8 methyl groups/molecule; HSD, 1.9 H, 3.4 methyl; Nugget, 2.3 H, 3.0 methyl; and Kentucky, 1.9 H, 2.6 methyl. Within the accuracy of the method, all

of the alcohols appear to be primary, as expected from the nature of the oxo reaction. In general, the number of branched methyl groups increases with the average carbon number of the alcohol mixture. As a comparison with some other, more highly branched, commercially-produced oxo alcohols, C_{13} -alcohols made from triisobutylene would have at least 6 methyl groups/molecule; those made from tetrapropylene would have at least 4 methyl groups/molecule; and C_{17} -alcohols made from tetraisobutylene would have at least 8 methyl groups/molecule.

Determination of Olefin Content of Mixtures by Using $C^{14}O$

If a mixture containing olefins is reacted with $H_2 + C^{14}O$, to a good approximation, each molecule of olefin will react with one molecule of CO , and therefore each olefin will be "tagged" with radioactivity. This will be true whether the olefin ends up as an alcohol, aldehyde, ester, ether, etc. The only exception is when the olefin hydrogenates to form the paraffin, and this is an important reaction under oxo conditions only for highly branched olefins, or compounds such as indene.

By measuring the radioactivity of the total oxo product obtained from each olefin-containing fraction relative to the radioactivity of the residual CO in equilibrium with the bomb contents at the end of the run, the initial olefin content of the mixture can be determined. In each 100 molecules of the olefin-containing mixture, where x molecules are olefinic, and Y is the average carbon number of the mixture;

$$\frac{x}{100 Y + x} \text{ (radioactivity of gas in bomb at end of run) = (radioactivity of product).}$$

Table 2 gives the results obtained by this procedure. Agreement between

TABLE 2.-Determination of olefin content of mixtures
by using $C^{14}O$

Mixture	Assumed average carbon number	Olefin Content, mole percent	
		Known	Found
Decene-1 + 1-methylnaphthalene)	10.0	47 50	52 56
Decene-1 + dodecene-1) + limonene +) 4-methylcyclohexene-1) + 1-methylnaphthalene)	9.5	55	53
HSF	12.4	$\frac{1}{40-55}$	55, 48
HSD	16.8	$\frac{1}{40-50}$	53, 42

1/ See table 1.

known and found values is satisfactory. Further work is being done on the other tar fractions, and on improving the accuracy of this analytical procedure.

ACKNOWLEDGMENTS

The authors wish to thank R. A. Friedel and A. G. Sharkey, Jr., for the spectrometric analyses; and P. Pantages for his technical assistance. The Nugget tar sample was obtained from Willis Beckering, U. S. Bureau of Mines, Grand Forks, North Dakota. The tar sample from the Kentucky hvab (high splint) coal was obtained from Bruce Naugle, U. S. Bureau of Mines, Pittsburgh, Pa.

REFERENCES

1. Wender, I., H. W. Sternberg, and M. Orchin. The Oxo Reaction. Ch. 2 in *Catalysis*, v. 5, ed. by P. H. Emmett, Reinhold Pub. Corp., New York, N. Y., 1957.
2. Aluminum Co. of America and Texas Power & Light Co. On Stream Prototype Solvent Extraction Plant for Lignite Tar. Texas Power & Light Co., P. O. Box 6331, Dallas 22, Texas.
3. Batchelder, H. R., R. B. Filbert, Jr., and W. H. Mink. Processing Low Temperature Lignite Tar. *Ind. and Eng. Chem.*, v. 52, 1960, pp. 131-136.
4. Kahler, E. J., D. C. Rowlands, J. Brewer, W. H. Powell and W. C. Ellis. Characterization of Components in Low-temperature Lignite Tar. *J. Chem. and Eng. Data*, v. 5, 1960, pp. 94-97.
5. Alekseeva, K. A., D. M. Rudkovskii, M. I. Ryskin, and A. G. Trifel. Preparation of High Molecular Weight Alcohols from the Products of Catalytic Coking by the Oxo Synthesis Method. *Khim. i. Tekhnol. Topliva i Masel*, v. 4, No. 5, 1959, pp. 14-18. Translation by Associated Technical Services, Inc., East Orange, N. J.
6. Rottig, W. Separation of Aliphatic Alcohols from Hydrocarbon-Alcohol Mixtures. U. S. Patent 2,746,984, May 22, 1956.
7. Société belge de l'azote et des produits chimiques du Marly, S. A. Continuous Separation of Higher Fatty Alcohols from Mixtures Containing Hydrocarbons. Belgian Patent 541,333, March 15, 1956; *Chem. Abs.*, v. 54, 1960, 16877e.
8. Washburn, R. M., E. Levens, C. F. Albright, and F. A. Billig. Preparation, Properties, and Uses of Borate Esters. Chap. in *Metal-Organic Compounds*, *Adv. in Chemistry Series*, v. 23, Am. Chem. Soc., Washington, D. C., 1959, pp. 129-157.

9. Zahn, C., A. G. Sharkey, Jr., and I. Wender. Determination of Alcohols by Their Trimethylsilyl Ethers. BuMines Rept. of Inv. 5976, 1962, 33 pp.
10. Kochloefl, K., P. Schneider, R. Rericha, M. Horák and V. Bazant. Isoprenoid-skeleton hydrocarbons in low-temperature brown coal tar. Chem. and Ind. (London), April 27, 1963, p. 692.
11. Bendoraitis, J. G., B. L. Brown, and L. S. Hepner. Isoprenoid hydrocarbons in petroleum - Isolation of 2,6,10,14-tetramethylpentadecane by high temperature gas-liquid chromatography. Anal. Chem., v. 34, 1962, pp. 49-53.

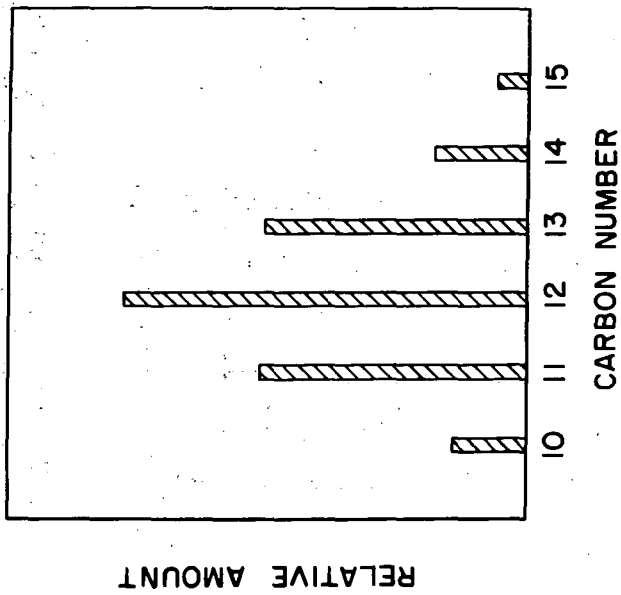


Figure 1.-Distribution of alcohols produced from hexane solubles foreruns fraction of Rockdale lignite tar.

L-8036 4-19-63

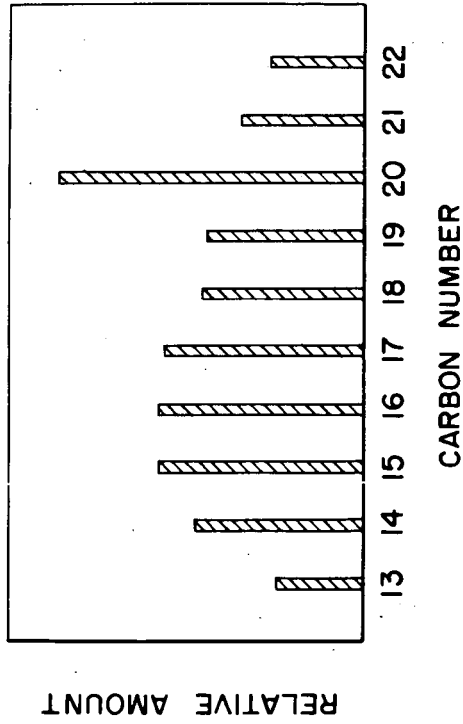


Figure 2.-Distribution of alcohols produced from hexane solubles distillate fraction of Rockdale lignite tar.

L-8037 4-19-63

11-6-63 L-8363

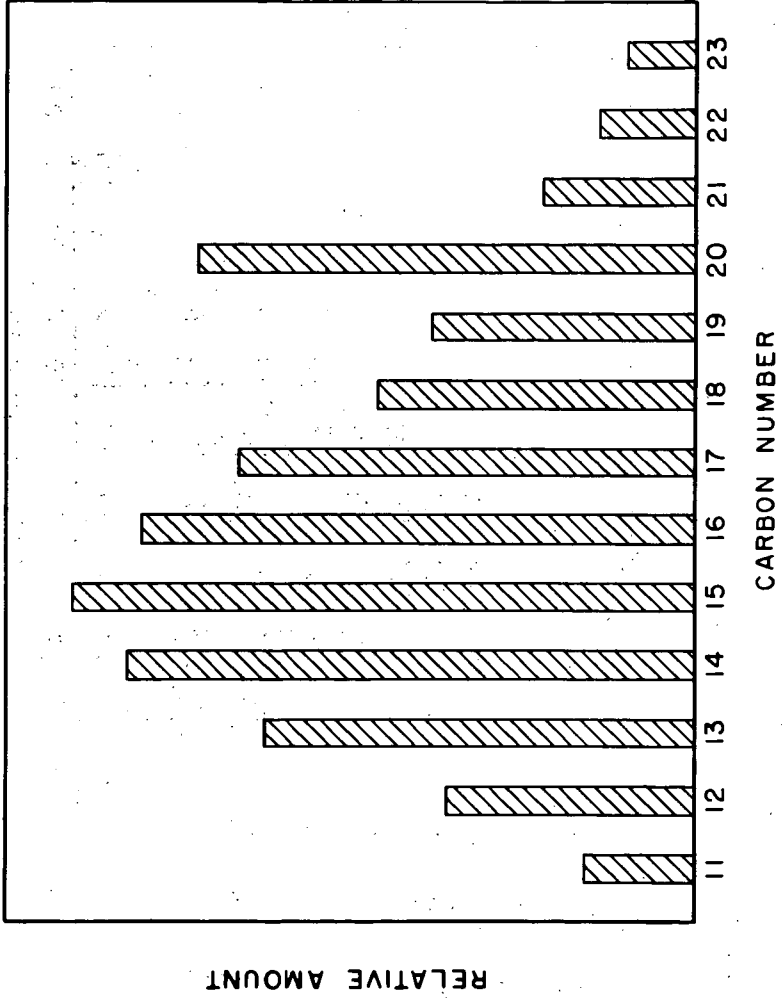


Figure 3. - Distribution of alcohols from nugget tar neutral oil produced from a Wyoming hvcb-suba coal.

11-6-63 L-8362

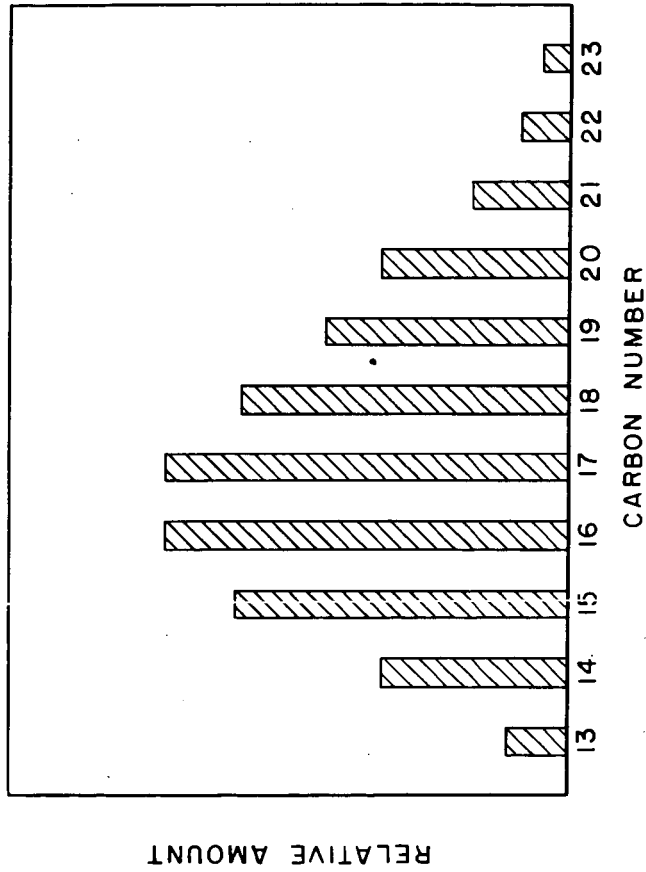


Figure 4. - Distribution of alcohols from a low-temperature tar neutral oil produced from a Kentucky hvab (high splint) coal.

Isolation of Porphyrins From Shale Oil and Oil Shale

J. R. Morandi and H. B. Jensen

Bureau of Mines, U.S. Department of the Interior
Laramie, Wyo.

INTRODUCTION

Oil shale is a laminated rock of sedimentary origin that ranges from gray to dark brown to almost black. It owes its color to carbonaceous matter called "kerogen" which is derived from plant and animal remains (1). Kerogen is largely insoluble in common organic solvents, but when heated to about 900°F it yields shale oil. This shale oil resembles petroleum in that it is composed of hydrocarbons and sulfur-, nitrogen-, and oxygen-derivatives of hydrocarbons.

The discovery of porphyrins in petroleum and oil shale by Treibs (12, 13) in 1934 gave direct evidence for the organic origin of petroleum and oil shales. In 1953 Groennings (5) published a method for extracting and spectrophotometrically determining porphyrins in petroleum. Groennings' procedure stimulated the work on the analysis of porphyrins in natural products. In 1954 Moore and Dunning (8) extracted Green River oil shale with various solvents and obtained a number of extracts that contained porphyrin-metal complexes. They concluded that the majority of the porphyrin exists in the shale as an iron-porphyrin complex. Although these researchers have reported the occurrence of porphyrins in oil shale, no one has reported their presence in shale oil. The present work was undertaken to determine if porphyrins were able to survive the retorting step and if so, what changes were brought about by retorting.

It was found in this investigation that:

- (1) Porphyrins are present in shale oil so they survive the retorting step.
- (2) Retorting changes the porphyrins from phyllo to etio type, and their average molecular weight is lowered. This lowering of the molecular weight is partially accounted for by decarboxylation.
- (3) Porphyrins present in shale oil are shown to be a complex mixture of predominantly etio type with an average of nine methylene substituents on the porphine ring. The absorption spectrum of the purest porphyrin prepared was nearly identical to the spectrum of a synthesized etio-type porphyrin.

EXPERIMENTAL WORK

Method of Extracting Porphyrins

Groennings' method (5) for the extraction of porphyrins was used with two modifications: (1) To reduce loss of porphyrins to the organic phase, a 20 percent

hydrochloric acid solution was used instead of the recommended 7 percent solution, and (2) to minimize decomposition of the porphyrin by contact with halogenated solvents (2) the final transfer of the porphyrins was made into benzene instead of into chloroform.

Source of Materials Studied

The oil shale studied was from the Mahogany Ledge of the Green River formation near Rifle, Colo. The shale contained 35 weight percent organic matter and assayed 64.3 gallons of oil per ton by the Modified Fischer assay method (10). Because the shale contained approximately 10 percent by weight of CO₂ as mineral carbonates, it was pretreated with 4 percent hydrochloric acid and air-dried prior to the porphyrin extraction step.

The crude shale oil was produced in an internally fired retort. The feed shale for this retort was also from the Mahogany Ledge of the Green River formation and averaged about 30 gallons of oil per ton. Selected properties of the oil, using the Bureau of Mines shale-oil assay method (11), were specific gravity, 0.950; weight percent nitrogen, 2.11; weight percent sulfur, 0.88; and a distillation analysis of 4.6 volume percent naphtha, 14.3 volume percent light distillate, 26.7 volume percent heavy distillate, and 54.3 volume percent residuum.

Spectral Procedures

The absorption spectra from 450 to 650 mμ of all porphyrin extracts, concentrates, and reference compounds were obtained in benzene solution. The method of Dunning (2) was used for correcting for background absorption in determining the type and quantity of porphyrins. The spectral reference compounds used in this research were mesoporphyrin IX dimethylester and etioporphyrin I.

Low-ionizing-voltage and high-ionizing-voltage mass spectra were obtained on selected extracts and concentrates. When a nickel complex of a porphyrin sample was introduced into the mass spectrometer, the spectrum obtained was of the nickel complex. The introduction of uncomplexed porphyrins resulted in the spectrum of the indium chloride complex of the porphyrins.^{1/} In both cases the mass spectra will be discussed as the spectra of the uncomplexed porphyrins.

Extraction and Concentration of Porphyrins From Shale Oil

Small-Scale Extraction

A 100-gram sample of the crude shale oil was extracted using the modified Groenings' method. This extract was purified by chromatographing it on a column containing 100 grams of activated alumina. Benzene was used to prewet the alumina and as the initial eluent. Benzene elution was continued until the solvent was almost colorless. Spectral examination of the benzene showed that no porphyrins were

^{1/} The indium chloride in the instrument resulted from the reaction of indium used for the valves in the sample introduction system and chlorine from chlorinated solvents used in other mass spectral projects.

removed. The porphyrin band was removed from the column using 1,2-dichloroethane, and elution with this solvent was continued until no porphyrins were discernible in the eluent. Visible absorption spectra were obtained on the extract before and after the chromatographic step. Low- and high-voltage mass spectra were obtained on the chromatographically purified extract.

Large-Scale Extraction

To obtain enough porphyrin extract for a characterization study, 2,300 grams of crude shale oil was extracted by the modified Groennings' method. The extract was chromatographed on 1,000 grams of activated alumina. Benzene was used to prewet the column and to elute the colored impurities, as was done on the small-scale experiment. The porphyrins were slowly eluted, using first recycled benzene and then mixtures of benzene and 1,2-dichloroethane. Twenty fractions were collected using benzene and 11 using benzene containing increasing quantities of 1,2-dichloroethane. Visible absorption spectra were obtained on all fractions, and mass spectra were obtained on selected fractions.

Countercurrent extraction was used as an additional separation on several of the fractions from the large-scale chromatographic separation. In each case, cyclohexane and 0.25 N hydrochloric acid were used as the immiscible solvents and 100 transfers were made. Absorption data were used to determine the distribution of porphyrins in the 100 tubes. Each time the separation was into four areas with concentration maxima occurring near tubes 33, 55, 75, and 95. The porphyrins in the tubes in each of the concentration areas were combined, and mass and absorption spectra were obtained on the recovered porphyrins.

Extraction of Porphyrins From Oil Shale

A sample of the hydrochloric acid leached shale, containing 105 grams of organic matter, was placed in a glass bomb, and 300 ml of benzene was added as a dispersant. The modified Groennings' extraction procedure was used to extract the porphyrins, except that the bomb was shaken continuously during the extraction. Visible absorption and mass spectra were obtained on the resulting extract.

RESULTS AND DISCUSSION

Porphyrin is the term applied to a class of compounds in which four pyrrole rings are united by bridge carbons to form a conjugated, macrocyclic structure, known as porphine. Figure 1 shows the numbering system that will be used in this paper for the porphine ring (9). This conjugated ring system is heat stable and can be halogenated, nitrated, or sublimed without destroying the macrocyclic structure (4).

Porphyrins, dissolved in organic solvents, have a typical, four-banded absorption spectrum in the visible region between 450 and 650 m μ . They have been classified into etio, phyllo, and rhodo types according to the height of the individual peaks relative to one another (3). Representative spectra of each of these three types are shown in figure 2. The four bands or peaks are numbered I, II, III, and IV starting from the long-wavelength end of the spectrum. In general, the height of the peaks increases toward the shorter wavelengths.

Porphyrins that have methyl, ethyl, vinyl, propionic acid, or hydrogen in positions 2, 3, 7, 8, 12, 13, 17, and 18 (see figure 1) around the porphine ring

give the etio-type spectrum. This etio-type spectrum, which is characteristic of blood-pigment porphyrins, has four peaks, which become progressively higher proceeding from the longer to the shorter wavelengths. The shale-oil extracts and concentrates gave etio-type spectra.

The phyllo-type spectrum, which is typical of the chlorophyll porphyrins, has peak II larger than III. This type of spectrum has been attributed either to the presence of an isocyclic ring between one of the pyrrole rings and the adjacent bridge carbon atom or to an alkyl group on one of the bridge carbon atoms. The oil-shale extracts gave phyllo-type spectra.

The rhodo-type spectrum has been observed in compounds having a carbonyl group attached to one of the pyrrole rings and has the number III peak as the strongest of the four main peaks. The rhodo-type spectrum was not observed for any of the oil-shale or shale-oil extracts.

The porphyrins in the extract from oil shale were characterized by the use of absorption and mass spectra. The absorption spectrum of this oil-shale extract is shown in figure 3. This spectrum is characteristic of phyllo-type porphyrin, which has peak II higher than peak III.

The low-voltage mass spectrum showed porphyrins with molecular weights from 462 to 536. The ions in this spectrum were in the three following homologous series: (1) The alkyl-substituted porphine series, (2) the series two mass units greater than the porphine series, and (3) the series two mass units less than the porphine series. Figure 4 shows the distribution of intensities of the ions for the series occurring at two mass units greater than the porphine series. The average molecular weight of the porphyrins in this series (as calculated from this distribution) is 508. More than half of the total ions in the low-voltage spectrum were in this series, and the data presented in figure 4 represent the three series.

In the high-voltage spectrum of the oil-shale extract there was a series of ions 44 mass units less than the parent ions. This series of ions was shown to be a fragment ion series corresponding to the loss of CO_2 from the porphyrins.

These characterization data show the following facts about the oil-shale porphyrins:

- (1) Oil-shale porphyrins are composed of at least three homologous series of compounds with no fewer than six different compounds in each series.
- (2) The majority of these compounds have a phyllo-type spectrum.
- (3) Some of these porphyrins have carboxyl substituents.
- (4) The average molecular weight of 508 for the oil-shale porphyrins can be accounted for by 1 carboxyl and 11 methylene substituents on the porphine ring.

Before the porphyrins from the small-scale extraction of shale oil could be characterized, it was necessary to remove some of the impurities carried along by Groennings' extraction. This was done by chromatographing on alumina, and the absorption spectra of the porphyrin extract before and after chromatography are shown in figure 5. Improvement in the purity of the porphyrins by the chromatographic step is shown by the smaller background absorption in the chromatographed concentrate. The shale-oil extract both before and after chromatographing gave an etio-type spectrum, whereas the oil-shale extract showed a phyllo-type spectrum.

In the low-voltage mass spectrum of the shale-oil extract, more than 90 percent of the parent ions were in the alkyl-substituted porphine series. Figure 6 shows the distribution of the ions in this series with molecular weight range from 366 to 492. The abscissa scale shows both m/e of the ions (molecular weights) and the number of methylene substituents necessary on the porphine ring to have this molecular weight. The average molecular weight of the porphyrins in shale oil (as calculated from this distribution) is 436, or the equivalent of nine methylene substituents on the porphine ring.

In the high-voltage spectrum of the shale-oil extract, there was no evidence of a fragment ion series 44 mass units less than the parent ions. This indicates that there are no carboxyl groups present in shale-oil porphyrins.

These characterization data show that shale-oil porphyrins are predominantly alkyl-substituted porphines with 4 to 13 methylene groups per molecule. Because the absorption spectrum of this extract is of the etio type, these alkyl substituents are on the eight pyrrole carbons in the porphine ring.

Comparison of the character of the porphyrins from oil shale with the character of the porphyrins from shale oil indicates the changes that porphyrins undergo during retorting. These changes are as follows:

- (1) The molecular weight is lowered an average of 72 mass units. In part, this is explained by decarboxylation. The decrease in average molecular weight is equivalent to the loss of one carboxyl and two methylene groups per molecule.
- (2) The phyllo-type character is changed to an etio-type character. The reaction necessary to bring about this change in spectral type is the removal of substituents from the bridge carbons on the porphine ring. This could also contribute to the lowering of the molecular weight of the porphyrins.

Further characterization of the porphyrins in shale oil was accomplished by examining the fractions from the chromatographic separation of the large-scale shale-oil extraction. The absorption spectra of the first 25 fractions from this chromatographic separation were of the etio type, and these fractions contained 70 percent of the total porphyrins recovered. Beginning with the 26th fraction, the height of peak II relative to peak III became increasingly greater. This indicated that some phyllo-type porphyrins were being eluted with the 1,2-dichloroethane. This presence of a phyllo-type porphyrin in the shale-oil extract is an indication that a part of the porphyrins is relatively unchanged during retorting.

A benzene-eluted fraction was used to demonstrate further the character of the etio-type porphyrins in shale oil. A nickel complex of the 15th fraction was prepared, and low- and high-voltage mass spectra of this complex were obtained. The peak heights in these spectra were corrected for isotope contribution. Figure 7a is the resulting low-voltage spectrum, and figure 7b is the resulting high-voltage spectrum. Each of the figures shows the corrected peaks only in the molecular weight region of the porphyrins.

The low-voltage mass spectrum has only ions in the porphine series. The number of substituents on the porphine ring is from 3 to 12 methylene groups with an average of 7 methylene substituents per molecule. The greater abundance of odd-numbered substituents over even-numbered is unexplained; this distribution is not evident in the low-voltage spectrum of the total shale-oil concentrate (see figure 5).

Hood (6) and Mead (7) have reported the mass spectral cracking pattern for metal complexes of etioporphyrin, and they concluded that the main fragmentation process is the loss of methyl groups. The peaks shown in figure 7b at one mass unit less than the porphine series could be due to the loss of methyl groups and indicate the presence of methyl or ethyl substituents on the porphine ring of shale-oil porphyrins.

The high-voltage spectrum of this fraction shows the presence of singly charged ions at every m/e from the molecular weight of the porphyrins to the doubly charged parent ions.^{2/} Both Hood and Mead have shown that in the mass spectrum of etioporphyrin I the porphyrin skeleton remains intact because no singly charged ions occur between the molecular weight of the porphyrin skeleton and the doubly charged parent ions. The conclusion, therefore, is that the fraction shows the presence of impurities. Because the low-voltage spectrum of this fraction showed no molecular ions other than porphyrins, the impurity is probably nonaromatic.

Countercurrent extraction was used to further purify the porphyrin concentrates. Fraction 14 from the large-scale chromatographic separation was countercurrent extracted and separated into four concentrates. Judging by the comparison of specific extinction coefficients, one of these concentrates was the purest porphyrin concentrate prepared in this work. That the impurity was still present can be seen by comparing the molar extinction coefficient (2) for this fraction which was 1.8×10^3 in benzene, with that for etioporphyrin I, which was 6.2×10^3 in benzene. This impurity, however, has low absorption in the visible region. This is illustrated by the good agreement of the visible spectrum of this concentrate with the spectrum of a synthesized etio-type porphyrin as shown in figure 8.

The low-voltage mass spectrum of the porphyrin concentrates from countercurrent extraction showed a series of molecular ions in the porphine series. One of the concentrates had parent ions occurring at molecular weights corresponding to four to eight methylene substituents on the porphine ring. Of the total parent ions present in the mass spectrum of this concentrate, 25 percent showed the presence of four methylene substituents, and 65 percent showed the presence of five methylene substituents.

CONCLUSION

This work has demonstrated that the skeleton of the porphyrin molecules in oil shale is capable of surviving retorting temperatures. However, the substituent groups on the skeleton are changed. As expected, reduction in average molecular weight is the most obvious change. Partial explanation of this reduction was demonstrated to be decarboxylation. Another change that can be inferred to take place is the removal of substituents responsible for the phyllo character of the oil-shale porphyrins. This could result either from the destruction of an isocyclic ring or from the removal of substituents from a bridge-carbon atom.

The porphyrins present in shale oil were shown to be a complex mixture of predominantly etio type. The absorption spectrum of the purest porphyrin prepared was nearly identical to the spectrum of a synthesized etio-type porphyrin. The porphyrins in shale oil have an average molecular weight equivalent to the porphine ring with nine carbon atoms of methylene substituents. The total number of carbon substituents ranged from 4 to 13.

^{2/} This was true for all extracts and concentrates prepared in this work.

ACKNOWLEDGMENTS

The work upon which this report is based was done under a cooperative agreement between the Bureau of Mines, U.S. Department of the Interior, and the University of Wyoming.

The authors wish to thank Dr. J. G. Erdman, Mellon Institute, for the samples of etioporphyrin I and mesoporphyrin IX dimethylester used in this research.

REFERENCES

- (1) Belser, Carl. Green River Oil-Shale Reserves of Northwestern Colorado. BuMines Rept. of Inv. 4769, 1951, 13 pp.
- (2) Dunning, H. N., J. W. Moore, and A. T. Meyers. Properties of Porphyrins in Petroleum. Ind. and Eng. Chem., v. 46, September 1954, pp. 2001-2007.
- (3) Fischer, H., and H. Orth. Die Chemie des Pyrroles (The Chemistry of the Pyrroles). Akademische Verlagsgesellschaft M.B.H., Leipzig, 1937; Edwards Bros., Inc., Ann Arbor, Mich., v. 2, pt. 1, 1943, pp. 579-587.
- (4) Goldstein, Jack M. Instrumental Studies of Porphyrin Compounds Obtained From Pyrrole Aldehyde Condensation. Ph. D. Dissertation, Univ. of Pennsylvania, 1959, 192 pp.
- (5) Groennings, Sigurd. Quantitative Determination of the Porphyrin Aggregate in Petroleum. Anal. Chem., v. 25, No. 6, June 1953, pp. 938-941.
- (6) Hood, A., J. G. Carlson, and M. J. O'Neal. Petroleum Oil Analysis. Ch. in The Encyclopedia of Spectroscopy, ed. by George W. Clark. Reinhold Publishing Corp., New York, N.Y., 1960, pp. 613-625.
- (7) Mead, W. L., and A. J. Wilde. Mass Spectrum of Vanadyl Etioporphyrin I. Chem. and Ind., August 19, 1961, pp. 1315-1316.
- (8) Moore, J. W., and H. N. Dunning. Interfacial Activities and Porphyrin Contents of Oil-Shale Extracts. Ind. and Eng. Chem., v. 47, July 1955, 1440 pp.
- (9) Patterson, Austin M., Leonard T. Capell, and Donald F. Walker. The Ring Index. McGregor and Werner, Inc., 1960.
- (10) Stanfield, K. E., and I. C. Frost. Method of Assaying Oil Shales by a Modified Fischer Retort. BuMines Rept. of Inv. 4477, 1949, 13 pp.
- (11) Stevens, R. F., G. U. Dinneen, and John S. Ball. Analysis of Crude Shale Oil. BuMines Rept. of Inv. 4898, 1952, 20 pp.
- (12) Treibs, A., Uber das Vorkommen von Chlorophyllderivaten en eines Olschiefer aus der oberen Triss (Occurrence of Chlorophyll Derivatives in an Oil Shale From the Upper Triassic). Ann. Chem. Liebigs, v. 509, 1934, pp. 103-114.
- (13) _____. (Chlorophyll and Hemin Derivatives in Bituminous Rock, Petroleum, Coals, and Phosphate Rock.) Ann. Chem. Liebigs, v. 517, 1935, pp. 172-196.

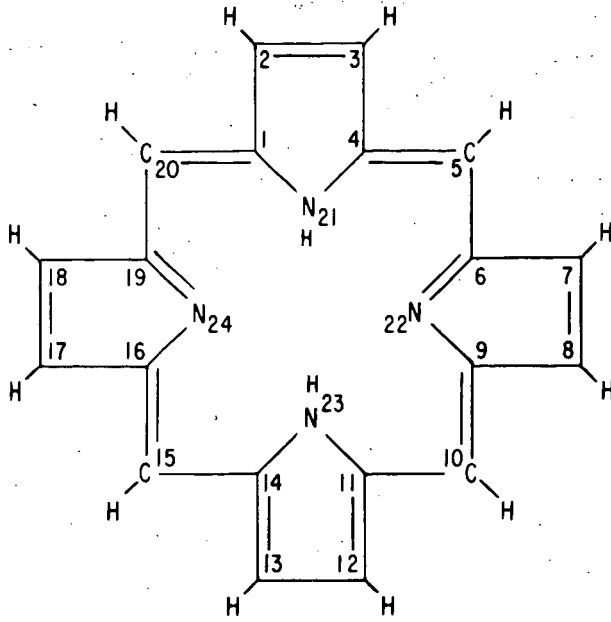
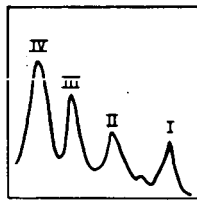
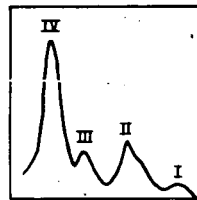


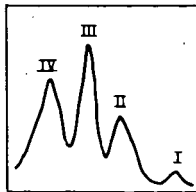
FIGURE 1-Numbering system for the Porphine Ring



ETIO



PHYLLO



RHODO

FIGURE 2-Types of Porphyrin Spectra.

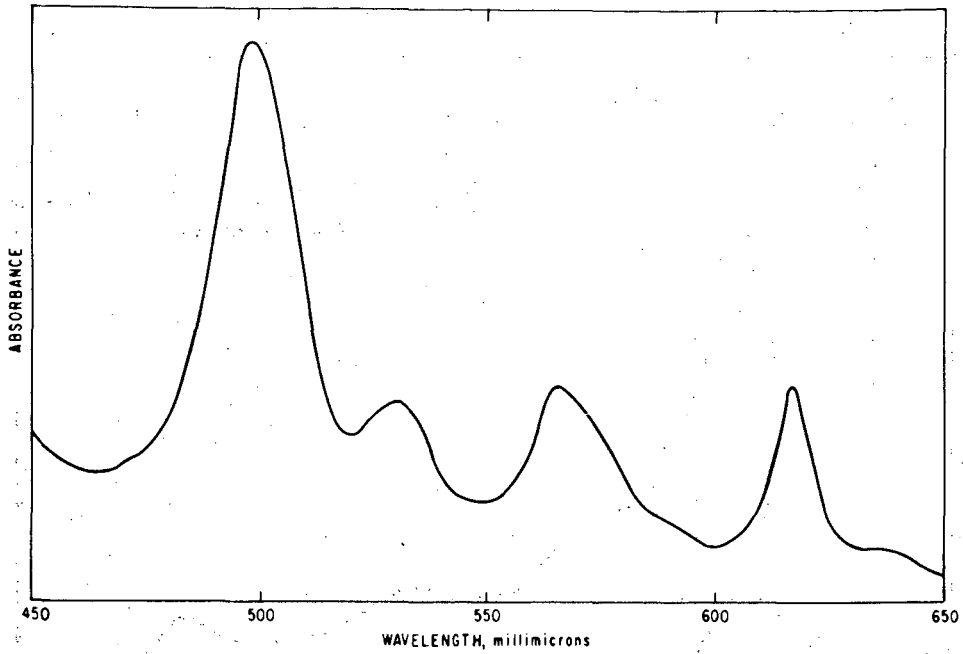


FIGURE 3-Spectrum of oil-shale extract

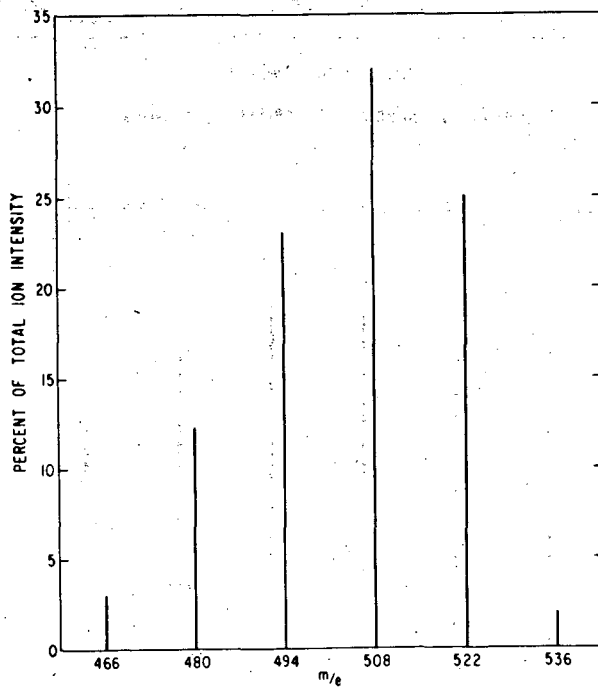


FIGURE 4-Distributions of ion intensities for oil-shale porphyrins

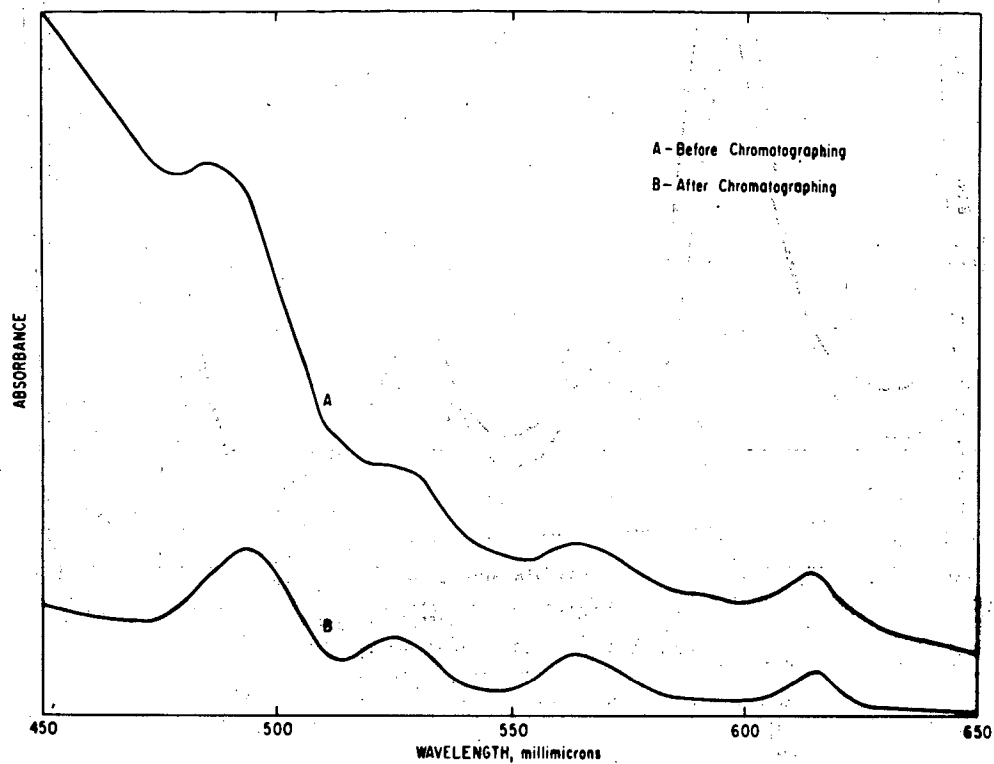


FIGURE 5.-Spectra of shale-oil porphyrins

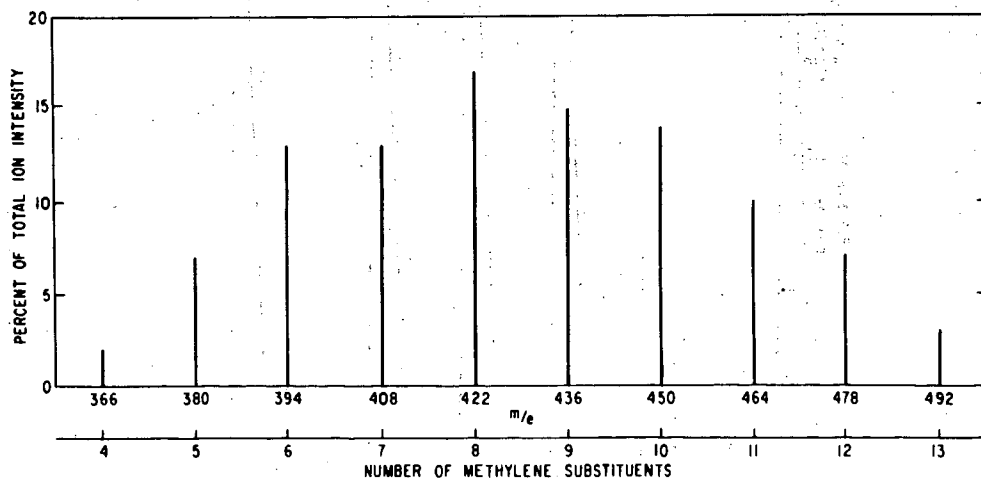


FIGURE 6.-Distribution of ion intensities for shale-oil porphyrins

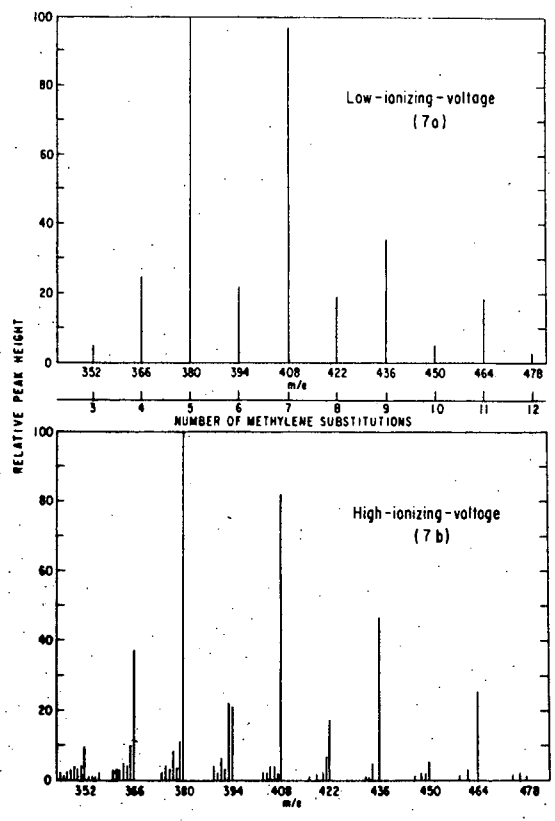


FIGURE 7: Mass Spectra of Fraction 15.

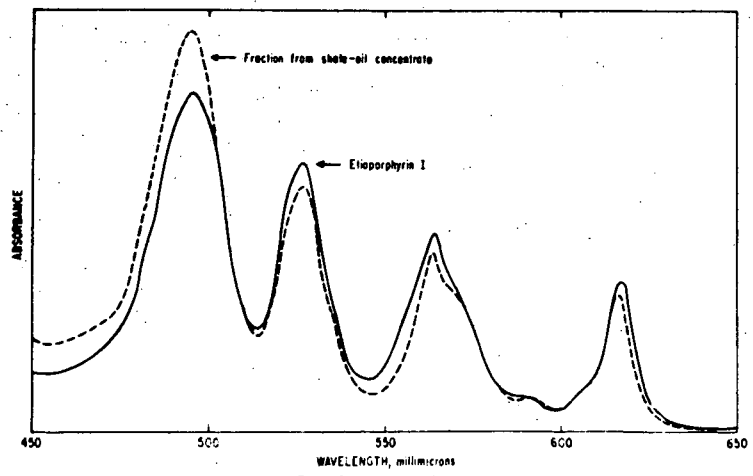


FIGURE 8: Comparison of spectra